



Advanced Fiber Materials for Wearable Electronics

Chuang Zhu^{1,2} · Jiawei Wu² · Jianhua Yan² · Xuqing Liu¹

Received: 9 July 2022 / Accepted: 11 September 2022 / Published online: 13 October 2022
© The Author(s) 2022

Abstract

Fiber materials are highly desirable for wearable electronics that are expected to be flexible and stretchable. Compared with rigid and planar electronic devices, fiber-based wearable electronics provide significant advantages in terms of flexibility, stretchability and breathability, and they are considered as the pioneers in the new generation of soft wearables. The convergence of textile science, electronic engineering and nanotechnology has made it feasible to build electronic functions on fibers and maintain them during wear. Over the last few years, fiber-shaped wearable electronics with desired designability and integration features have been intensively explored and developed. As an indispensable part and cornerstone of flexible wearable devices, fibers are of great significance. Herein, the research progress of advanced fiber materials is reviewed, which mainly includes various material preparations, fabrication technologies and representative studies on different wearable applications. Finally, key challenges and future directions of fiber materials and wearable electronics are examined along with an analysis of possible solutions.

Keywords Conductive fibers · Piezoelectric fibers · Sensors · Artificial muscles · Energy harvesting and storage

Introduction

In recent years, there has been an increasing interest in wearable electronics that are made of fiber materials [1–4]. In contrast to their rigid counterparts, fiber-based wearable electronics hold great promises for the next generation of electronic devices because they are flexible and stretchable [5–7]. Fibers are ideal to be explored as the platform for the next generation of wearable electronics as they can be converted into conformable clothing through well-established and cost-effective textile production methods [8–11]. Furthermore, the hierarchical nature (fiber-yarn-fabric-product) of these fibrous assemblies makes it particularly suitable for the fabrication of wearable electronics. Basically, there are many favorable attributes of fiber assemblies. Mechanically, they have good flexibility to deform under stretching,

bending, twisting and shearing, and own outstanding ability to maintain structural integrity during washing. Moreover, when a large deformation is applied in the fiber assemblies, the induced internal strain in the fibers is very small, indicating the excellent fatigue resistance. Also, there is no crack propagation in the fiber assemblies because the large number of fibers in the assemblies play the role of crack arrestors to prevent catastrophic failure of the structure, demonstrating the superior damage tolerance. Thermally, they exhibit high porosity and large surface area to trap still air as insulators in cold climate and allow hot air to escape from human body in hot weather. In addition, the thin and porous structure of fiber assemblies endows electronic devices with breathability, which is a major concern for the comfort of wearables [12]. On the other hand, it is scientifically proven and technically feasible to build electronic functions including sensing, actuating, communicating and computing on fibers, accelerating the advancement of fiber-shaped wearable electronics such as flexible circuits [13], fabric antennas [14], conformal sensors [15] and fiber-enabled actuators [16].

To transform these concepts into engineering prototypes, the most important consideration is the fabrication of fiber materials that have the ability to fulfill the performance requirements of fiber-based wearable electronics [17]. Fibers have been used in human lives for hundreds of

✉ Xuqing Liu
xuqing.liu@manchester.ac.uk

¹ Department of Materials, School of Natural Sciences, University of Manchester, Oxford Rd, Manchester M13 9PL, UK

² Key Laboratory of Textile Science & Technology, Ministry of Education, College of Textiles, Donghua University, Shanghai 201620, People's Republic of China

years since the emergence of woven textiles from natural fibers such as cotton, hemp, silk and wool [18]. Following the development of chemistry and improvement of fiber industry technology, synthetic fibers such as polyamide [19], polyester [20] and polyurethane (PU) [21] have been manufactured. Unlike natural fibers, the length, thickness and color of chemical fibers can be specifically tailored to meet different end uses of fiber products [22]. In the information age, with the progress of material science and nanotechnology, functional fibers that have special functions such as electrical conductivity, piezoelectric effect and thermoelectric performance have been studied extensively [23–25]. Recently, with the combination of methods of different academic disciplines, smart fibers with energy harvesting and storage, sensing, shape deformable and chromatic-changeable characteristics have been developed and opened up the research of fiber-based wearable electronics [26–28].

Although tremendous efforts have been spent on the design of fiber-enabled wearable electronics, most reported results are still far from practical applications owing to technical hindrances [29]. Herein, the material selection for functional fibers, fabrication techniques, electronic components, devices and application of fiber-shaped wearable electronics are systematically reviewed. An attempt will be made to review critically the numerous publications in the literature and discussions will also be presented regarding to limitations of current fiber materials and wearable electronics with respect to manufacturability and practicality that must be resolved and improved prior to their wide adoption.

Conductive Fibers for Wearable Electronics

The functionality of fiber-based electronic devices highly relies on the electrical performance of fibers and it can be said without exaggeration that the good electrical conductivity of fiber-shaped wearable electronics is equivalent to the stable blood circulation in humans [30]. Therefore, conductive fibers that support high carrier mobility and have good overall electrical conductivity, together with desirable mechanical and environmental stability, are the most important component of the fiber-based wearable electronics. This section will focus on the discussion of conductive fibers (Fig. 1). First, the main types of the involved conductive materials (metals, conducting polymers, carbon-based materials, liquid metals and MXene) will be investigated. Second, the fabrication methods of conductive fibers including coating, fiber making and structural transformation will be reviewed. Then, applications of conductive fibers in wearable electronics including sensors, supercapacitors, batteries and artificial mussels will be discussed.

Conductive Materials

One important consideration for conductive fibers is the choice of conductive materials with excellent electrical performance, good mechanical properties, reliable safety and superior environmental stability [43]. The basic principle of electing conductive candidates is that they have no negative effect on the original performance of textile fibers [44]. According to the elemental compositions and conductive mechanisms, the present frequently used conductive materials for the fabrication of conductive fibers are broadly categorized into the following five groups: metals, conductive polymers, carbon-based materials, liquid metals and MXene.

Metal

Traditional metallic materials are the most widely employed conductive elements in the engineering field due to their high conductivity and low price. For example, the normalized conductivity/cost ratio of nickel (Ni) (1.4×10^{-2}) is much higher than graphite (8×10^{-4}) [45]. In order to facilitate practical usages of metals in fiber-based wearable electronics, bulk metals are designed into the shapes of thin wires. However, metal wires are stiff and rigid, limiting their applications in wearables which require adequate flexibility and deformability. Recently, low-dimensional nanostructures of metals such as nanoflakes, nanowires (NWs) and nanoparticles are particularly attractive for manufacturing conductive fibers [46]. Compared with block metals, an excellent bonding interaction between metallic nanomaterials and fibers is provided by the nanoscale-sized nanostructures, and the surface energy and surface tension are increased because of the high aspect ratio. Low-dimensional metals can be coated on or incorporated in fibers through sputtering, electrodeposition and wet spinning. Among various metallic nanomaterials, metal NWs such as silver (Ag) NWs [47], gold (Au) NWs [48] and copper (Cu) NWs [49] have drawn much attention in terms of thermal/electrical conductivity, mechanical strength and flexibility. Metal NWs are compatible with low-cost solution-based processing including spin coating, spray coating and inkjet printing, which makes them suitable for the scale-up production. Owing to the mesh-like percolating structures, the electrical performance of metal NWs is similar to bulk metals while consuming a substantially low quantity of raw materials. To realize the advantages and large-scale applications of metal NWs, it is very essential to overcome the high electrical resistance between the wire junctions that leads to poor thermal uniformity and the ease of oxidation when exposed to harsh environments [50].

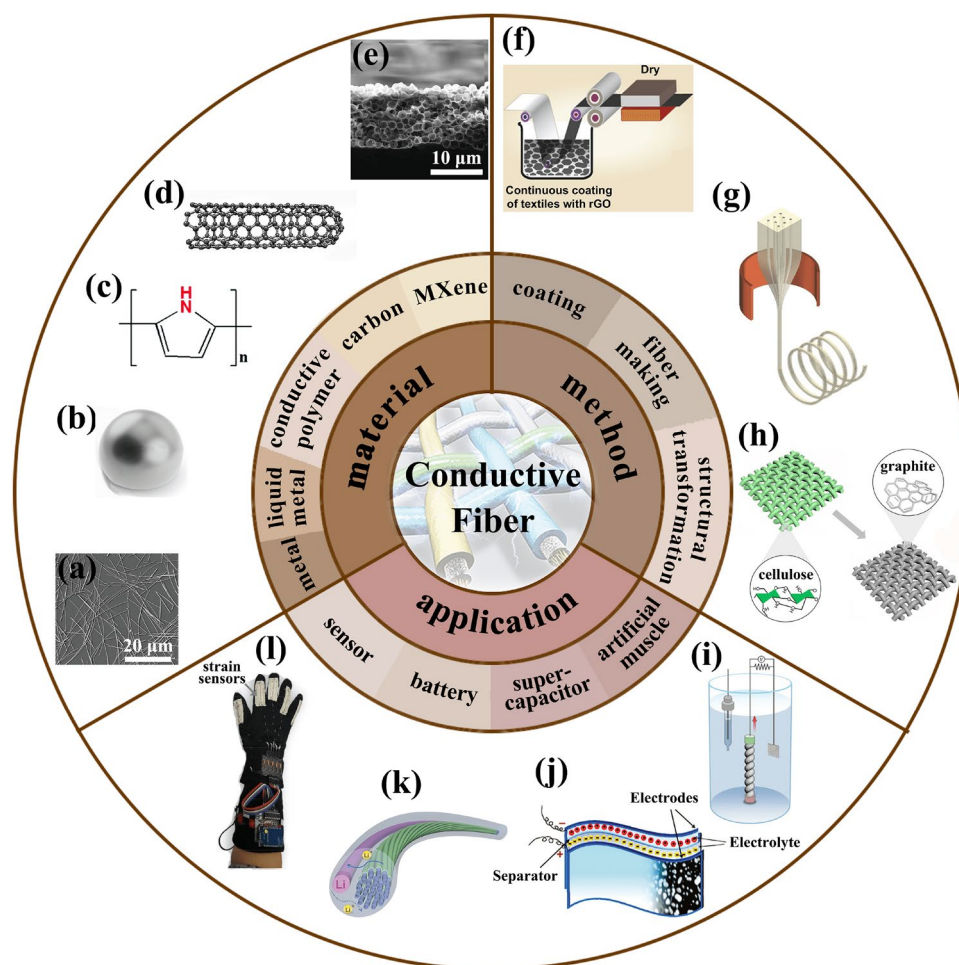


Fig. 1 **a** Scanning electronic microscope (SEM) image of silver nanowires; reproduced with permission from Ref. [31], Copyright 2017, American Chemical Society. **b** Photograph of liquid metal; reproduced with permission from Ref. [32], Copyright 2021, American Chemical Society. **c** Chemical structure of polypyrrole; reproduced with permission from Ref. [33], Copyright 2015, Royal Society of Chemistry. **d** Model of carbon nanotube (CNT); reproduced with permission from Ref. [34], Copyright 2012, Royal Society of Chemistry. **e** SEM image of $\text{Ti}_3\text{C}_2\text{T}_x$ film; reproduced with permission from Ref. [35], Copyright 2017, Wiley-VCH. **f** Fabrication process of graphene-coated fabrics; reproduced with permission from Ref. [36], Copyright 2017, American Chemical Society. **g** Thermal drawing process for manufacturing conductive fibers; reproduced with

permission from Ref. [37], Copyright 2018, Wiley-VCH. **h** Carbonization procedure for producing conductive fabrics; reproduced with permission from Ref. [38], Copyright 2021, Elsevier. **i** Fiber-based artificial muscle; reproduced with permission from Ref. [39], Copyright 2017, American Association for the Advancement of Science (AAAS). **j** Supercapacitor made of graphene/polypyrrole coated fabric electrodes; reproduced with permission from Ref. [40], Copyright 2011, American Chemical Society. **k** Lithium-ion battery based on the aligned multi-wall CNT/Si composite fiber; reproduced with permission from Ref. [41], Copyright 2013, Wiley-VCH. **l** Image of a fiber-based strain sensor; reproduced with permission from Ref. [42], Copyright 2017, American Chemical Society

Conductive Polymer

Since the discovery that doping can be used to make conjugated polymers conductive, there has been an increasing interest in the field of intrinsically conductive polymers (ICPs). Unlike most organic polymers that are electrically insulating, ICPs can be tuned to have specially tailored electronic, electrical, magnetic and optical properties by molecular design of basic building blocks. Based on this, a tremendous amount of research work has been conducted to develop ICPs and investigate their applications in transistors,

supercapacitors and field emission display. The oxidized π -conjugated system in which polarons and bipolarons are mobile in an electric field is responsible for the electrical conduction of ICPs. Theoretically, the conductivity of ICPs can reach up to 2×10^9 S/m when all charged dopants are spatially removed from the quasi-one-dimensional conduction pathway [51]. However, in the real situation, the electrical conductivities of most ICPs are in fact in the same range as those of inorganic semiconductors due to their low degree of crystallinity and many other defects. To achieve high conductivity of ICPs, the key is to improve the mobility

of charge carriers. Up to date, a large number of ICPs have been discovered, including polypyrrole (PPy), polyaniline (PAni), polythiophene (PTh), polyacetylene (PAC) and poly[3,4-(ethylenedioxy)thiophene]:poly(styrenesulfonate) (PEDOT:PSS) [52]. Among these ICPs, PEDOT:PSS holds great promises due to its high conductivity, good optical transmission, superior processability and excellent water solubility [53]. There is a diverse array of strategies to integrate ICPs into conductive fibers. For example, by injecting the PEDOT:PSS solution into the CaCl_2 coagulation bath that is controlled by a syringe pump at certain flow rates, and then drawing of the solvent from the solution, the PEDOT fiber is formed and its electrical conductivity reaches 38 S/cm [54]. At present, the greatest challenge of ICPs for fiber-based electronic applications is their poor environmental and thermal stabilities.

Carbon-Based Material

Carbon-based materials have attracted unprecedented attention due to their large specific surface area, high electrical conductivity, good mechanical properties and superior environmental stability [55]. According to the structural dimensions, carbon-based materials are mainly divided into 0D carbon black particles, 1D carbon nanotubes (CNTs), 1D carbon fibers (including microfibers and nanofibers) and 2D graphene [56]. Among them, CNTs and graphene are the most intensively explored carbon allotropes in material science. CNTs can be categorized as single-walled (SWCNTs) and multi-walled (MWCNTs), and a MWCNT usually contains a number of concentric SWCNTs with inter-wall spacing of ca. 0.34 nm. Due to strong carbon–carbon covalent bonds and unique atomistic structures of CNTs, they exhibit excellent mechanical and physical properties [57]. For example, the elastic modulus and tensile strength of CNTs are in the order of 1.0 Tpa and 50 Gpa. Especially, the electrical conductivity of SWCNTs is as high as 10^8 S/m, which is higher than that of Cu [58]. However, due to the nonpolar structure of CNTs, they cannot be well dispersed in common solvents, making them difficult for the large-area application. In addition, CNTs tend to aggregate and even form large clusters because of their high aspect ratio and strong van der Waals attraction. To solve these problems, it is crucial to develop suitable solvents for the fabrication of high-performance CNT-based conductive fibers. Graphene, consisting of a hexagonal honeycomb lattice of carbon atoms in sp^2 hybridized orbitals, has received a lot attention from both of scientific studies and technological development due to its exceptional electric, mechanical and chemical properties. Graphene made by mechanical exfoliation and chemical reduction is high conductive but its dispersion in polar solvents is poor owing to the inherently inert surface [59]. Instead, graphene oxide (GO) that contains oxygen groups

on its surface can be fully dissolved in most solvents such as water, acetone, ethanol and ethylene glycol, making it suitable for solution processing. Furthermore, a series of thermally or chemically reduced process can be used to enhance the relatively poor electrical conductivity of GO, resulting in the formation of reduced GO (rGO) [60].

Liquid Metal

Among various conductive materials, liquid metals (LMs) that can maintain liquid state at room temperature hold a special place since they possess both metallic and amorphous properties that belong to solid metals and water-like fluids [61]. This kind of material refers to elemental metals and their alloys compounded with other ingredients that are used to further reduce decrease the melting point. It is well known that there are five traditional metals in the nature can be defined as LMs: mercury (Hg, -39 °C), francium (Fr, -27 °C), cesium (Cs, 28.4 °C), gallium (Ga, 29.8 °C) and rubidium (Rb, 38.89 °C) [62]. As emerging functional materials, Ga-based LMs not only show metallic attributes such as high electrical conductivity, superior thermal conductivity and good corrosion resistance, but also retain liquid characteristics including excellent fluidity, superb flexibility and low viscosity. For example, when the environmental condition is at 20 °C, the viscosity of eutectic gallium-indium (EGaIn) is twice that of water. In particular, the nonvolatile EGaIn is less toxic than Hg and exhibits no radioactivity in comparison with Rb, Cs and Fr. What is more, the high chemical stability of EGaIn promotes its harmlessness and biocompatibility [63]. In general, Ga-based LMs include pure Ga, EGaIn, gallium-indium-stannum ternary alloy (GaInSn) and gallium-indium-stannum-zinc quaternary alloy (GaInSnZn) and they have kept attracting great attentions over a wide variety of promising applications, such as textile circuits, high-contrast imaging, drug delivery and 3D printing [64]. Nevertheless, such materials still encounter many practical challenges due to the inherent limitations of macroscopic LMs. For example, the resolution of fabric circuits fabricated by bulk LMs is relatively low. By sintering conductive traces that are made of LM nanoparticles, the resolution of constructed circuits can be effectively improved. Thus, scaling down the physical size of LMs is crucial for broadening their applications in flexible printed electronics.

MXene

MXene, as a class of new-born 2D materials, has gained tremendous attention by the research community since the first report of Ti_3C_2 by Gogotsi et al. [65]. MXenes are metal carbides and nitrides featuring a framework containing two or more layers of transition metal atoms that

are packed into a honeycomb-like 2D lattice, which are intervened by carbon and/or nitrogen layers occupying the octahedral sites between the neighboring transition metal layers [66, 67]. The general formula of MXene flakes is $M_{n+1}X_nT_x$ ($n = 1-3$ and x is variable), where M represents the transition metal site, X means carbon and/or nitrogen sites and T stands for terminated functionalities such as $-O$, $-OH$, $-F$ and $-Cl$ on the surface of the outer transition metal layer. For example, the chemical formula of a titanium carbide MXene with two layers of transition metal ($n = 1$), which is completely oxygen-terminated, can be written as Ti_2CO_2 . MXenes are usually synthesized by using a top-down method, in which selective etching is applied to remove A-layer atoms (e.g., Al, Si and Ga) from the $M_{n+1}AX_n$ phase precursors that consist of a pack of layered, hexagonal-architecture ternary carbides and nitrides, leading to the formation of stacked MX layers, which can be further exfoliated into single-layer flakes [68, 69]. Due to tunable surface termination, metallic conductivity, outstanding dispersibility in aqueous solutions, unique layered structure and large specific surface area, MXenes are endowed with great potentiality in various application fields including wearable electronics, energy storage and biomedicine. Especially, the high electrical conductivity (1.5×10^6 S/m), solution processability and ease of fabrication process of MXene render it as a promising material to convert conventional textiles into conductive fibers [70]. Despite that, several drawbacks of MXenes, such as poor stability at oxygen atmosphere, low mechanical flexibility and easy restacking, limit the further development of highly desired flexibility and durability of flexible wearable electronics. Therefore, developing MXene-based composites with admirable flexibility is the crucial for the boost of fiber-shaped wearable devices.

Fabrication Technologies to Conductive Fibers

After making a general understanding of the frequently used conductive elements for smart fibers, the next question is naturally raised that how to impose these conductive materials into fiber systems [71]. Due to complex material properties, uneven surface morphologies and variable curved structures of textiles, the good combination between conductive materials and textile systems is a big challenge [72]. Therefore, providing the most convenient and economic approach to accomplish an excellent compatibility with existing textile technologies is the key for large-scale application of conductive elements. The common preparation techniques of fabricating conductive fibers mainly include coating, fiber making and structural transformation.

Coating

Coating, as one of the most common methods for producing conductive fibers, refers to a surface treatment that forms a conductive layer with a nano- to micro-scale thickness on the surface of a fibrous material by means of an auxiliary tool [73]. In the composite fiber, the inner fiber substrate plays the role of soft backbone to provide flexibility, while the outer conductive coating layer serves as electron transport pathways. Importantly, a certain bond strength between coating materials and fibers is preferred because it can accommodate the subsequent application requirements by increasing the durability [74]. Therefore, the addition of a protective layer outside the conductive layer or the insertion of certain adhesives as the middle layer is usually required during the coating. Coating technique mainly include dip coating [75], spraying [76], screen printing [77], vacuum filtration [78] and electroless deposition (ELD) [79].

Dip-coating method is to completely immerse the non-conductive substrate into a certain concentration of uniformly dispersed conductive material liquid for some time, followed by washing and drying to form a homogeneous conductive layer on the substrate [80]. Although the consumption of conductive coating materials is large for the treatment of absorbent fibers, dip coating can form a more uniform conductive layer. As shown in Fig. 2a, Chen et al. reported a highly stretchable EGaIn fiber that consisted of stretchable PU as the core fiber layer, polymethacrylate (PMA) as the intermediate viscose modified layer and the EGaIn as the outer conductive layer via dip coating [81]. The obtained PU@PMA@EGaIn fiber showed excellent electrical conductivity (over 10^5 S/m) when stretched up to 500% strain.

ELD is an autocatalytic redox reaction in which metal cations in the metal salt solution are reduced into metallic nanoparticles and coated on the catalytic active surface sites of the substrate material [82]. Compared with physical vapor deposition, chemical vapor deposition and electrodeposition, ELD that needs no sophisticated equipment and external electricity is very attractive for fabricating conductive fibers. As shown in Fig. 2b, Chen et al proposed Ni-coated cotton yarns via ELD [83]. Because catalyst-based Ni seed crystals were caged by the topographical genus structures of cross-linked polyacrylamide, a highly electrically conductive interconnecting network ($3 \Omega/cm$) was formed and Ni-deposited yarns exhibited high durability against repeated 1500 cycles of folding and 5 cycles of washing.

Screen printing refers to the method of transferring conductive material through the mesh to the surface of the substrate material by the extrusion of the scraper [84]. Importantly, this strategy can be used to form conductive circuits on flexible substrates by selectively coating conductive nanoparticles on them. Furthermore, the equipment for screen

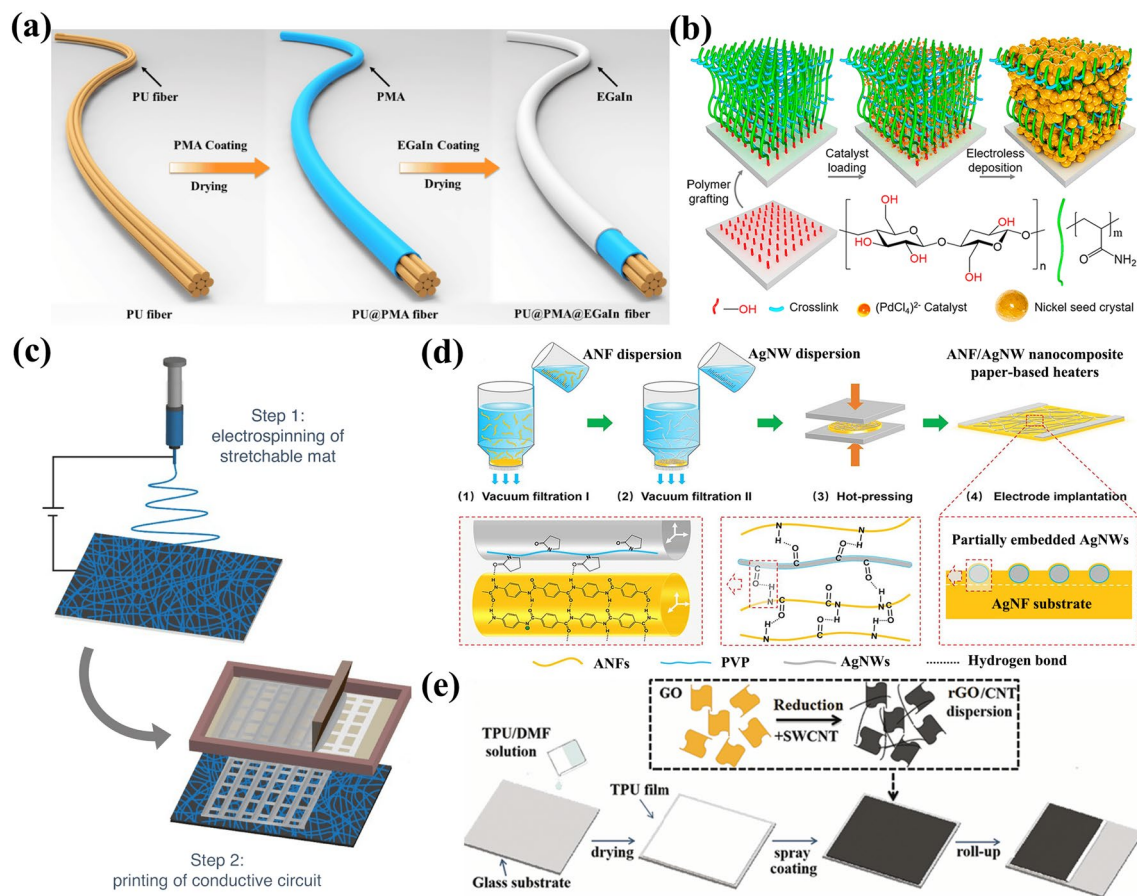


Fig. 2 **a** Schematic illustration showing the preparation process of the PU@PMA@EGaIn fiber via dip coating; reproduced with permission from Ref. [81], Copyright 2020, American Chemical Society. **b** Fabrication procedure of Ni-coated cotton yarns via ELD; reproduced with permission from Ref. [83], Copyright 2020, American Chemical Society. **c** Scheme of the process for the fabrication of screen-printed conductive stretchable mat; reproduced with permission from Ref.

[85], Copyright 2021, Springer Nature. **d** Synthesis procedure of the ANF/AgNW nanocomposite papers via vacuum filtration; reproduced with permission from Ref. [87], Copyright 2019, American Chemical Society. **e** Schematic diagram of the fabrication of SWCNT-rGO TPU yarns by using spraying; reproduced with permission from Ref. [89], Copyright 2020, Elsevier

printing is simple and easy to operate, and the process of printing is adaptable. As shown in Fig. 2c, Ma et al. reported the liquid–metal fiber mat (LMFM) that was fabricated by three simple steps: electrospinning of the poly(styrene-block-butadiene-block-styrene) (SBS) fiber mat with excellent elasticity, screen printing of EGaIn onto the stretchable fiber mat and activation of permeability on the LMFM via pre-stretching [85]. Importantly, the planar EGaIn was transformed into a laterally mesh-like and vertical wrinkled structure hanging among the SBS microfibers during the repeated stretching cycles. This unique framework endowed LMFM with high permeability, superior electrical stability, exceptional conductivity (up to 1.8×10^6 S/m), good biocompatibility and smart adaptiveness to omnidirectional stretching over 1800% strain.

Vacuum filtration is a technique in which conductive materials are forced to be separated from the liquid and

deposited on the surface of the substrate by taking advantage of the pressure difference formed through the vacuum pump inside and outside the collection bottle [86]. This method is usually used in water treatment systems and the laboratory vacuum filtration device only takes up a small footprint. As illustrated in Fig. 2d, Gu's group reported conductive nanocomposite papers based on the heat-resistant aramid nanofibers (ANFs) and high conductive AgNWs via two-step vacuum-assisted filtration and hot-pressing approach [87]. Benefitting from the bilayer structure, as-made nanocomposite papers presented low sheet resistance ($0.12 \Omega/\text{sq}$) and excellent heat resistance (thermal degradation temperature above 500°C).

Spraying is a common method that uses a high-pressure spray gun to atomize liquid conductive materials and then uniformly disperse them on the surface of the substrate material to form a conductive layer [88]. By using spraying,

the utilization of conductive materials can be effectively improved, resulting in the reduced cost. As demonstrated in Fig. 2e, Xie et al. developed a spirally layered CNT-graphene/PU composite yarn through spraying [89]. The addition of 2D rGO into 1D CNT network could significantly improve the electrical conductivity of the composite yarn (8 S/m) and the spirally layered structure endowed the conductive yarn with the large working strain of 620%.

Fiber Making

Fiber making is another efficient way to prepare conductive fibers and the common ones are mainly electrospinning [90], wet spinning [91], thermal drawing [92] and solution blow spinning [93]. Electrospinning is a straightforward and versatile method to draw charged threads from viscose polymer fluids or polymeric melts up to fibers that are in the diameter range from nano to the submicron range by using electric forces. Electrostatic spinning has attracted many researchers and gained much attention because of

its controllable process, versatility and easy production of continuous nanofiber from a wide variety of materials [94]. As shown in the Fig. 3a, Javed et al. reported conductive graphene-biopolymer nanofibrous fabrics by electrospinning the precursor that was made of GO nanoparticles as the source of graphene, 1-butyl-3-methylimidazolium chloride (BMIMCl) as the ionic liquid and cellulose acetate (CA) as the biopolymer [95]. These electro-spun nanofibers could be further reduced into CA-BMIMCl-rGO by using hydrazine vapor under ambient conditions and the electrical conductivity of such nanofibers increased from 2.71×10^{-5} to 5.3×10^{-1} S/m by adding only 0.43 wt.% of GO.

Thermal drawing is a method that consists of designing the architectures in a macroscopic scaled-up model of the fiber, heating of the preform in the furnace of the drawing tower, and the drawing of kilometers-long fibers by regulating the relationship between viscous force, internal stress and surface tension [96]. Thermal stretching demonstrates many advantages such as large-scale manufacturing, customizable structure and easy combination with other techniques.

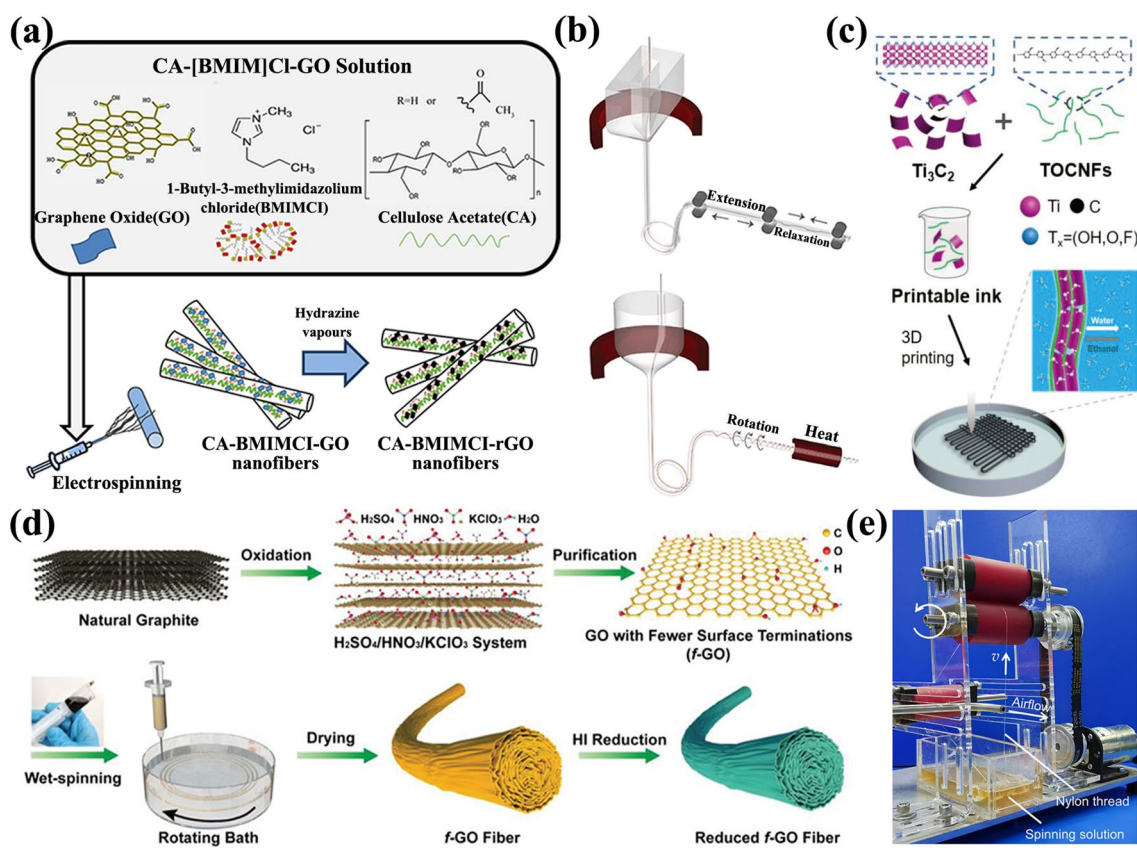


Fig. 3 a Schematic illustration of the preparation of CA-BMIMCl-rGO nanofibers via electrospinning; reproduced with permission from Ref. [95], Copyright 2018, Elsevier. b Scheme of the process for the fabrication of conductive yarns via thermal drawing; reproduced with permission from Ref. [97], Copyright 2022, Wiley-VCH. c Schematic diagram of the fabrication process of conductive fibers via 3D printing; reproduced with permission from Ref. [99], Copyright 2019, Wiley-VCH. d Scheme showing the preparation processes of reduced f-GO fiber via wet spinning; reproduced with permission from Ref. [101], Copyright 2022, Wiley-VCH. e Synthesis of nanofibers via needleshless SBS system; reproduced with permission from Ref. [103], Copyright 2022, AAAS

As shown in Fig. 3b, Marion et al. explored two approaches for manufacturing thermally drawn highly conductive fibers (10^7 S/m) with controlled elasticity [97]. First, a buckling instability was induced post draw to create a wavy path for the metal wire within a cavity of the thermally drawn elastomer fiber. Secondly, the cladding and the metal microwire were twisted simultaneously to create helical metal electrodes embedded in a stretchable yarn. The meandering and helical metal electrodes in thermally drawn fibers could reach 50% elongation while maintaining minimal change in resistance ($<0.5\%$).

3D printing refers to a parallel design and manufacturing technology that produces physical objects by adding selected materials layer by layer and following digital 3D model guidance [98]. This method has received a lot of attention and is also used in the research of fiber-based wearable electronics due to its advantages of high productivity, pollution-free manufacturing and customizability. As shown in Fig. 3c, Cao et al. reported the fabrication of flexible smart fibers and textiles by using a 3D printing technique with hybrid inks of (2,2,6,6-tetramethylpiperidine-1-oxylradical)-mediated oxidized cellulose nanofibrils (TOCNFs) and Ti_3C_2 MXene [99]. Due to the synergistic effect between the 1D TOCNFs (guiding the formation of macroscopic flexible fibers) and 2D Ti_3C_2 nanosheets (contributing to the electrical conductivity and photothermal conversion ability), as-prepared 3D-printed fibers exhibited significant responsiveness to multiple external stimuli (photon/electron). When the concentration of initial Ti_3C_2 nanosheets was 50 wt.%, the electrical conductivity of TOCNFs/ Ti_3C_2 fibers reached maximum (2.11×10^2 S/m).

Wet spinning strategy provides an approach that mainly includes extrusion of the polymer solution from the spinneret holes, deposition of the generated fibers inside a coagulation bath where the polymer precipitates and collection of the sample through the winding device [100]. The wet spinning process offers the advantage of manufacturing different fibers with various cross-sectional shapes and sizes. As shown in Fig. 3d, Tang et al. reported a scalable additive-free wet-spinning methodology for efficiently producing high-performance pristine graphene fibers by optimizing surface chemistry of GO nanosheets [101]. Compared with GO prepared by the conventional Hummers method (h-GO), GO fabricated by modified Staudenmaier approach contained fewer surface terminations (f-GO), especially trace carboxyl groups, which made it more readily to form liquid crystals for spinning and to construct compact and ordered alignment due to the stronger interlayer interactions. Benefiting from the low oxidation degree and the fewer irreparable defects, the thoroughly reduced f-GO fibers could afford an excellent electrical conductivity of 1.06×10^5 S/m.

In addition to the above-mentioned methods, solution blow spinning (SBS) approach opens a new window for

producing nanofibers [102]. In a typical SBS process, the solution is first refined by a gas flow-induced shearing force generated at the gas–liquid interface and then extruded from a needle tip. After forming a liquid jet along the streamwise direction, a gas flow effectively assists in solvent evaporation, leaving behind dry fibers. However, the needle-based SBS technique has some inherent limitations such as high flow resistance, droplet formation and ejection, and the needle blocking. To solve these problems, Li et al. devised a needless Kármán vortex SBS system in which a roll-to-roll nylon thread was used to deliver spinning solution, coupled with vertically blowing airflow to draw nanofibers, as shown in Fig. 3e [103]. This system could manufacture a wide variety of nanofibers including polymers, ceramics and carbon at a production rate of up to 5.90 g/hour per jet.

Structural Transformation

Structural transformation that mainly involves inducing defects implantation [104], carbonization [105] and laser direct writing [106] is an efficient and practical way to produce conductive fibers. Defects implantation is a method in which the electron bonding and band structure are tuned in variant degrees by different types of defects produced in various sites of metal oxides lattices, resulting in notable changes of metal oxides in optical, electrical, magnetic and thermal properties [107]. Among them, oxygen vacancies have attracted the worldwide research interest because oxygen-deficient metal oxides show significantly enhanced properties such as photoabsorption ability, electrical conductivity and electrocatalytic activity. As shown in Fig. 4a, Yan et al. fabricated conductive ceramic nanofiber textiles via oxygen vacancies implantation [108]. Different from high-temperature reduction to create defects, the self-driven chemical reaction was first used to induce oxygen defects in oxides at room temperature by putting dimethylacetamide-wetted TiO_2 textiles on lithium plates. The domino-cascade reduction from the interface to the whole textile was triggered by these defects to fulfill the transformation of oxide ceramic textiles from insulation to conduction (40 S/m).

Carbonization refers to a method that uses heat treatment to directly carbonize some natural and artificial fibers including cellulose, polyacrylonitrile and asphalt into carbon fibers with high electrical conductivity [109]. The carbonization technique has paved a new route for the fabrication of conductive fibers in a cost-effective manner. As shown in Fig. 4b, Yan et al. produced sponge-like porous carbon nanofibers via carbonization [110]. In the fabrication process, poly (vinyl alcohol) as the carbon precursor, boric acid as the crosslinking agent and poly (tetrafluoroethylene) as the pore inducer were firstly selected to form water-soluble webs, followed by electrospinning them into fibrous films. Finally, B-F-N triply doped porous carbon nanofibers with

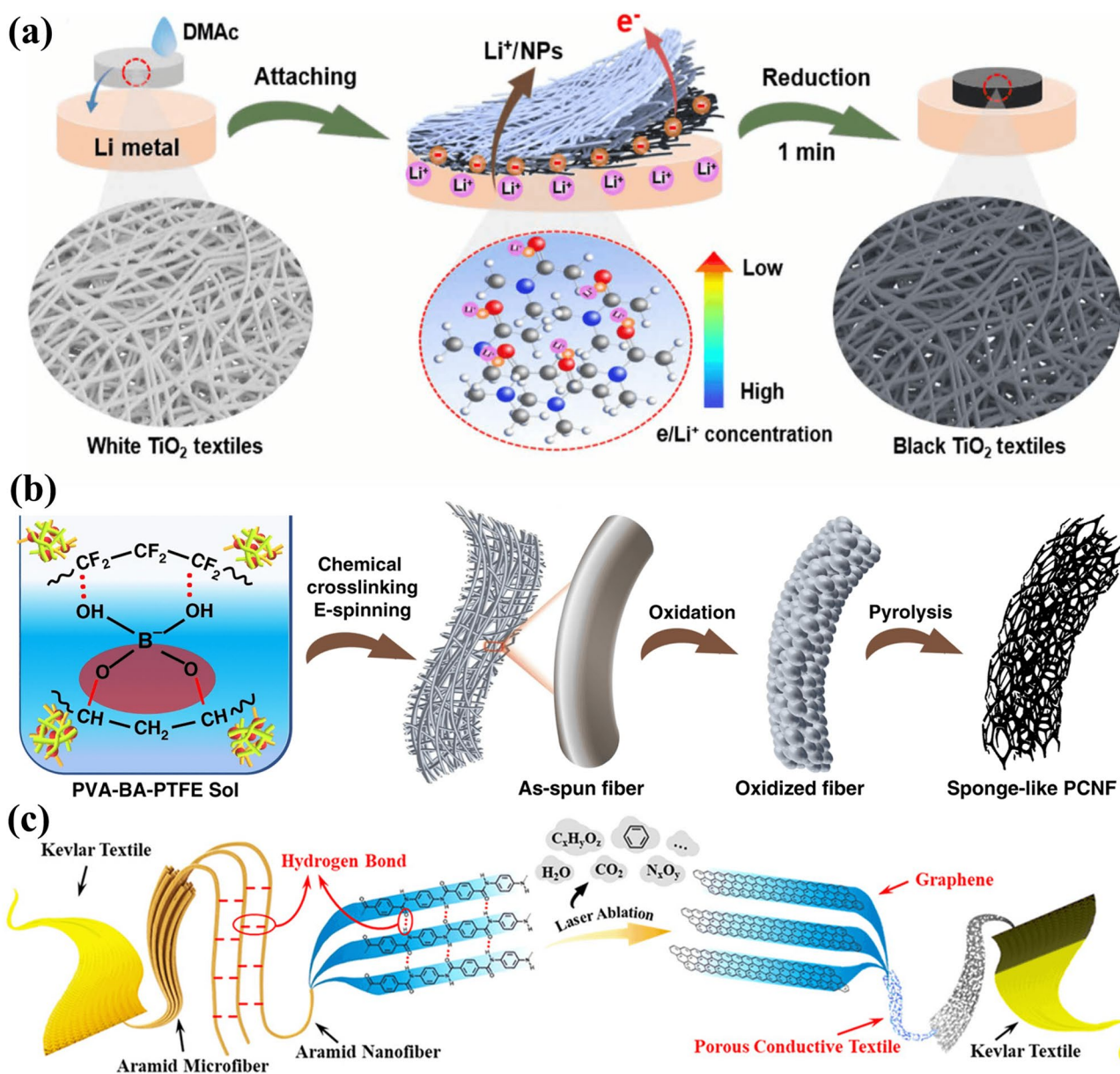


Fig. 4 **a** Schematic procedure of the fabrication of conductive TiO_2 textiles by inducing defects in oxides under room temperature; Reproduced with permission from Ref. [108], Copyright 2020, AAAS. **b** Schematic illustration of the fabrication process of conductive carbon nanofibers via carbonization; reproduced with permission from Ref.

[110], Copyright 2019, Springer Nature. **c** Schematic diagram of the formation of graphene on Kevlar fabrics via laser writing; reproduced with permission from Ref. [112], Copyright 2020, American Chemical Society

ultrahigh porosity of $> 80\%$ and outstanding conductivity of $9.8 \times 10^4 \text{ S/m}$ after oxidation and pyrolysis.

Laser direct writing refers to a molding approach in which a laser beam is used to directly structure the material surface without any physical contact [111]. This technique can process complex materials with a resolution spanning more than three orders of magnitude from millimeters to microns, which make it an effective tool for preparing conductive textiles. As shown in Fig. 4c, Wang et al. reported the

laser-induced transformation of Kevlar into a graphene-functionalized textile in air by using a CO_2 infrared laser [112]. During the direct laser scribing, the localized temperature on Kevlar was high due to the photothermal effect, leading to the broken $\text{C}=\text{O}$ and $\text{N}-\text{C}$ bonds, and the remaining carbon atoms were reorganized into graphene. The resistance of laser-induced graphene (sample size: $2 \times 0.5 \text{ cm}^2$) reached 10.6Ω when the laser power was 8.0 W.

Applications of Conductive Fibers in Wearable Electronics

As discussed, conductive fibers fabricated through careful selection of material composition and fabrication technology

are highly conductive, flexible and durable [113]. Therefore, they are very suitable for being used as electrodes and current collectors for fiber-based wearable electronics that demand simultaneous achievements of electronic functions and robust mechanical properties [114]. In the past few

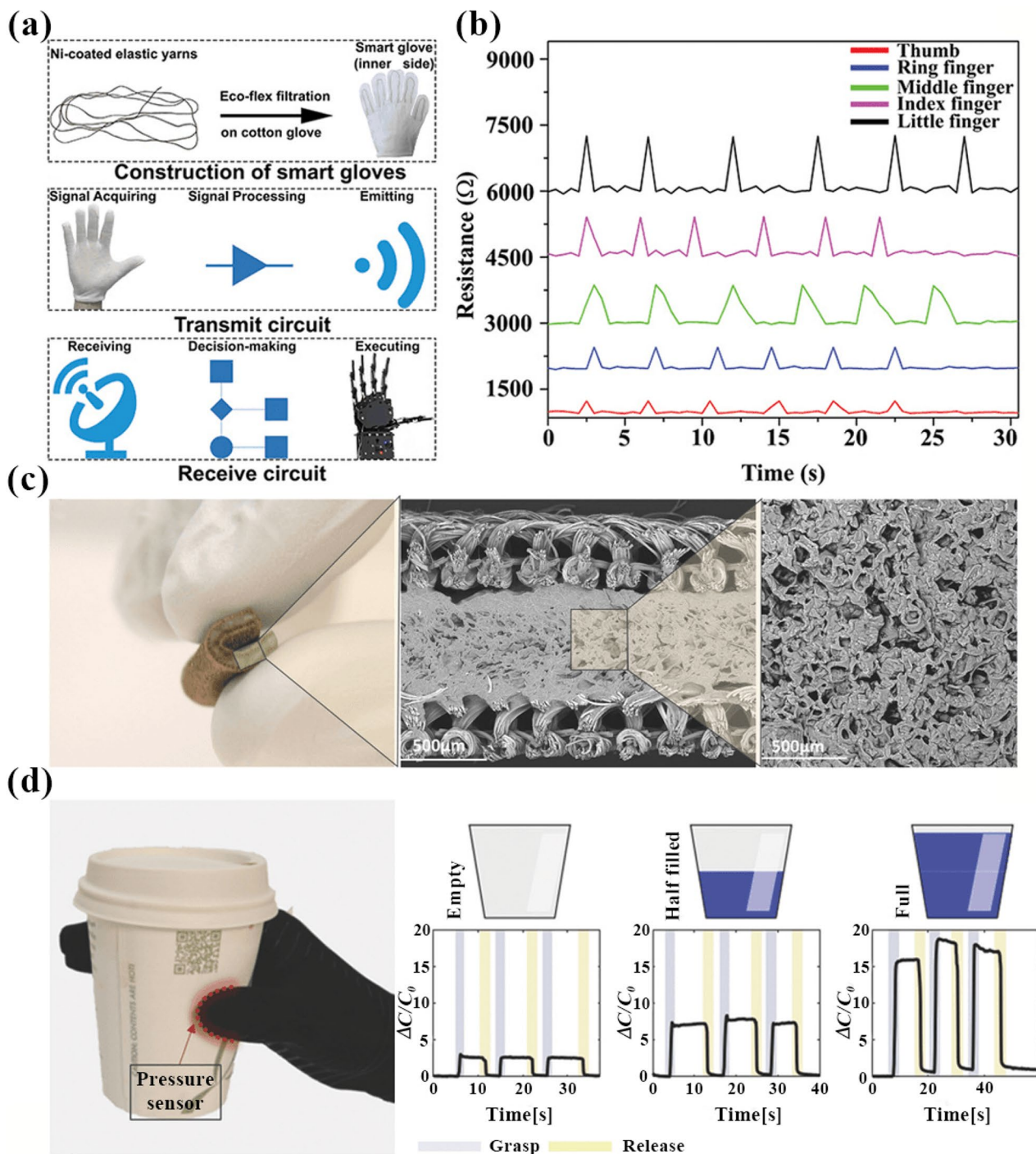


Fig. 5 **a** Schematic diagram of human–machine remote control system based on the yarn-based resistive sensor. **b** Real-time recoding of finger motions expressed in the form of resistance change. **a, b** Reproduced with permission from Ref. [124], Copyright 2020, Wiley-VCH. **c** Actual image

and cross-sectional SEM image of the flexible capacitive pressure sensor. **d** The graphics showing the change in capacitance when grasping different amount of weights. **c, d** Reproduced with permission from Ref. [126], Copyright 2017, Wiley-VCH

years, a wide range of electronic devices including sensors [115], artificial muscles [116], supercapacitors [117] and batteries [118] have been fabricated with superior performance and excellent flexibility/wearability.

Sensors

Conductive fibers can be directly integrated into wearable electronic devices as passive components to detect

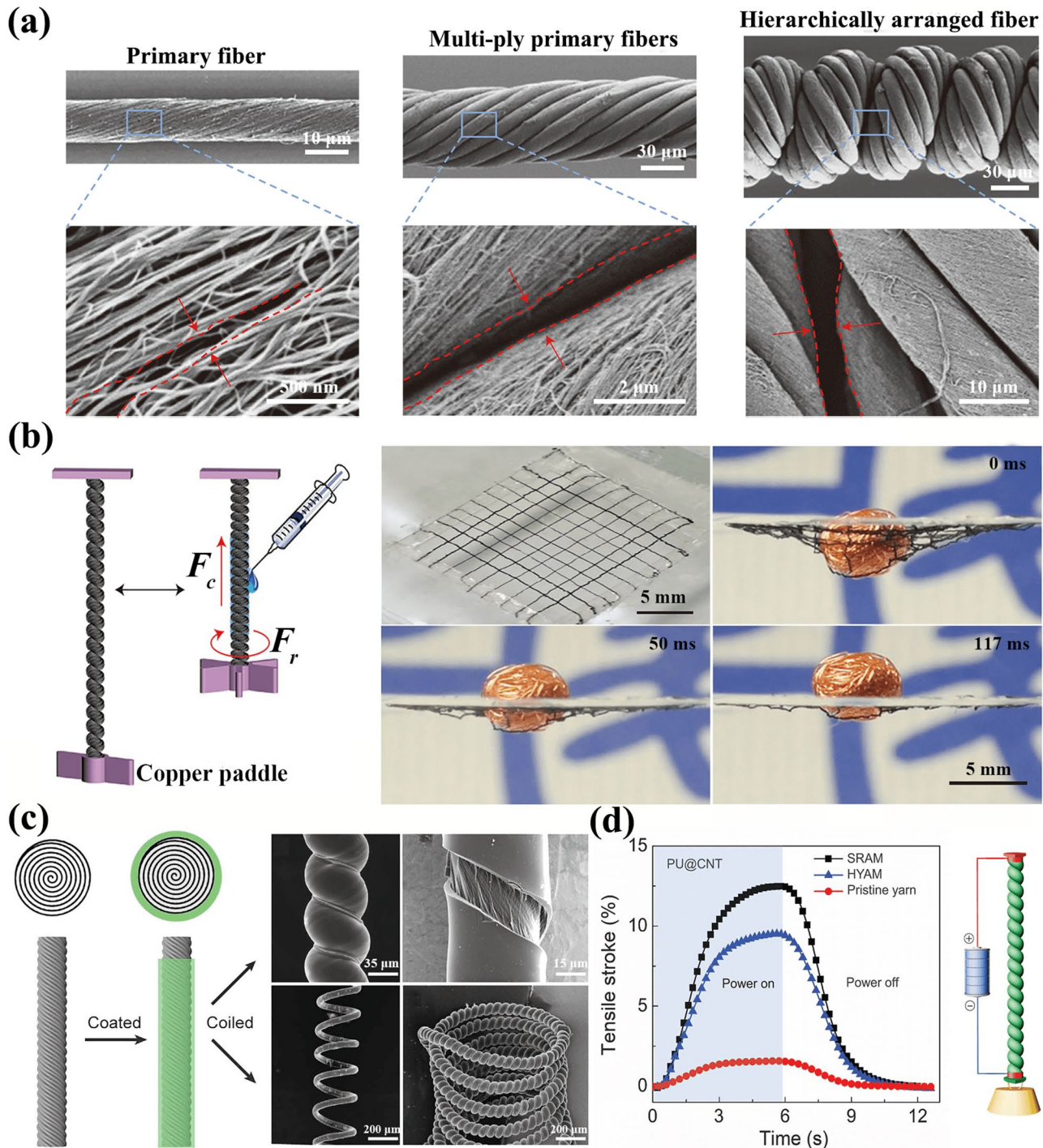


Fig. 6 **a** SEM images of CNT fibers in different states with the gap structure. **b** Schematic illustration of the contractive and rotary actuations of the HHF and their application in smart textiles for lifting a copper ball. **a, b** Reproduced with permission from Ref. [128], Copyright 2015, Springer Nature. **c** Schematic diagram of the fabrication

process of a typical SRAM and SEM image of various SRAMs. **d** Iso-baric tensile actuation of electrothermally powered SRAMs, HYAMs and pristine CNT yarns by using the illustrated configuration. **c, d** Reproduced with permission from Ref. [129], Copyright 2019, AAAS

mechanical stress/strain. Fiber-based wearable strain sensors are mainly classified into the following four categories: resistive [119], capacitive [120], piezoelectric [121] and triboelectric [122]. Among them, resistive and capacitive sensors have been studied extensively due to their high sensing reliability in dynamic conditions and excellent sensitivity

to identify extremely small strains. Resistive strain sensors are prepared with a layer of fiber-based electrodes and the working mechanism of these sensors relies on the strain effect, which means physical signal of mechanical deformation or the action of external force can be converted into the change of resistance through the sensitive material and

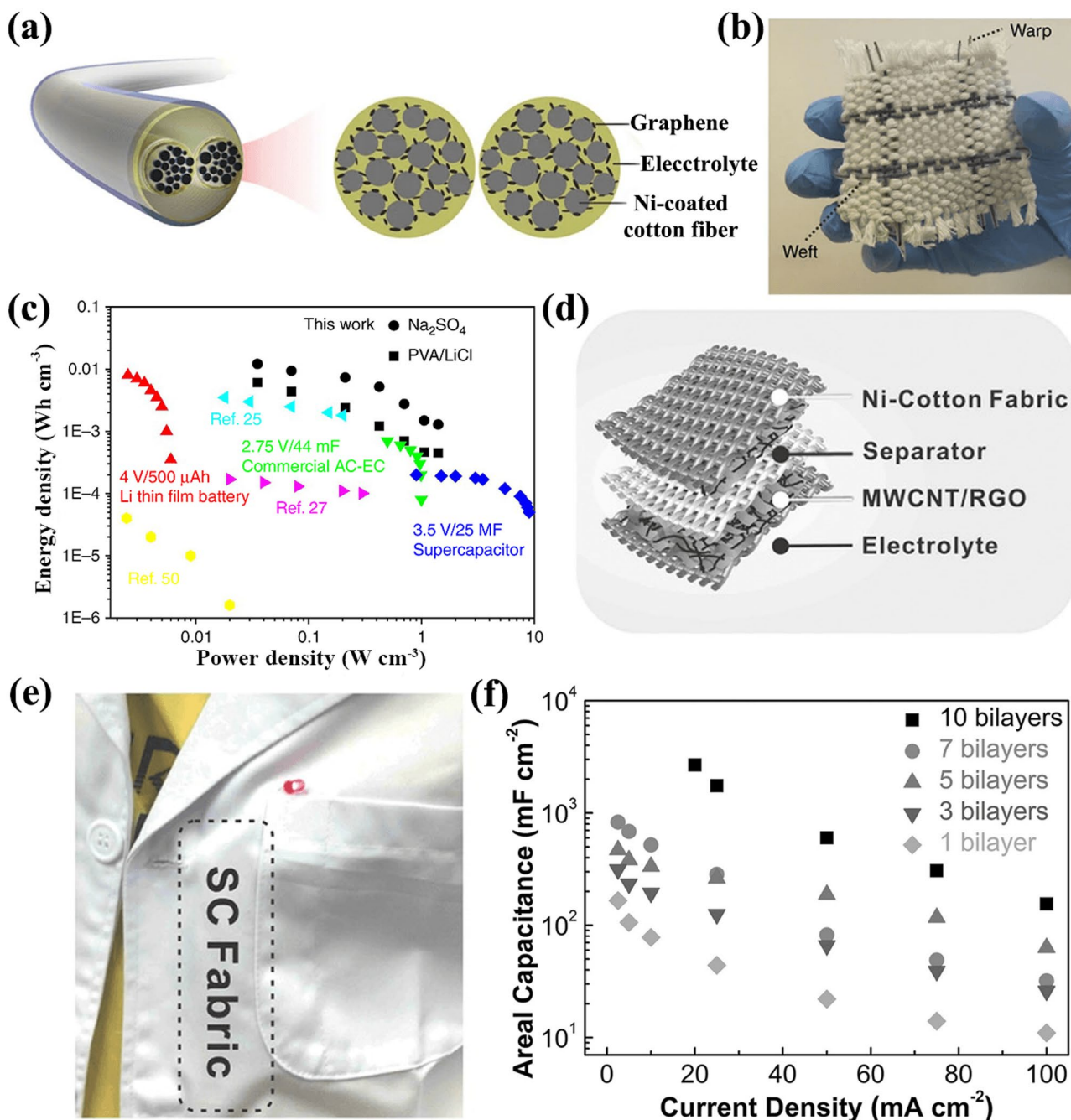


Fig. 7 **a** Schematic illustration of the structure of one supercapacitor yarn. **b** Digital image showing a woven fabric made of solid-state supercapacitor yarns. **c** Ragone graph of yarn-based supercapacitor and some commercial devices. **a–c** Reproduced with permission from Ref. [131], Copyright 2015, Springer Nature. **d** Schematic diagram of

fabric-based supercapacitor. **e** Digital image showing one supercapacitor fabric device that was sewn into a lab coat for powering the LED. **f** Areal capacitances of the composite fabric electrodes with different numbers of MWCN/rGO bilayers. **d–f** Reproduced with permission from Ref. [132], Copyright 2017, Wiley-VCH

the conversion element, followed by recording the signal change in real time via the measurement conversion circuit [123]. As shown in Fig. 5a, Zhu et al. proposed a resistive strain sensor by attaching conductive elastic yarns with Ni-coated nylon sheath and stretchable PU core to cotton glove via Ecoflex filtration, which played an important role in the overall control system consisting of transmit circuit and receive circuit [124]. During the bending/releasing motion of human fingers, less/more Ni-coated nylon wrappings were brought into contact, resulting in the increased/decreased resistance (Fig. 5b). Based on this, the finger motions could be monitored by the yarn-based sensors and through the signal processing units, these sensors were capable of controlling the robotic hand. Capacitive strain sensors are made of two fiber electrodes and a dielectric layer, forming a sandwich structure [125]. When applied with a certain voltage, opposite charges accumulate on the top and bottom electrode. However, the dielectric layer in the middle hampers the current transmission, leading to the whole structure acting as a capacitance. The value of capacitance depends on the overlap area between two electrodes, the thickness of the dielectric layer and the relative permittivity of the dielectric layer. As shown in Fig. 5c, Atalay et al. reported a capacitive-based soft pressure sensor with high sensitivity ($1.21 \times 10^{-2} \text{ kPa}^{-1}$) by laminating two conductive fabrics onto the microporous silicone elastomer as a dielectric layer [126]. By integrating such sensor into a textile structure to create a smart tactile glove, different weights could be detected by observing the change in capacitance because the induced pressure caused the varied thickness of the dielectric layer (Fig. 5d).

Artificial Muscles

Artificial muscle refers to a class of materials and devices that can reversibly contract, expand, or rotate within one component in respond to external stimuli, such as magnetic field, electricity, irradiation, heat and atmosphere. Conductive CNT fibers are ideal candidates for the fabrication of artificial muscles because they can be simultaneously drawn and twisted to form CNT yarns that are capable of providing fast, high-force, large-stroke torsional and tensile actuation [127]. For example, Chen et al. fabricated hierarchically arranged helical CNT fiber actuators [128]. As shown in Fig. 6a, MWCNT arrays synthesized through chemical vapor deposition were first dry-spun to form the primary fibers with a helical angle of $\sim 32^\circ$ and a diameter of $15 \mu\text{m}$ and there were a large number of gaps ranging from tens to hundreds of nanometers among the helically aligned MWCNTs. Afterwards, a twisting process was used to arrange these multiply primary fibers into a helical structure, in which micrometer-scale gaps were formed among neighboring primary fibers. Finally, the first coil was developed when

the inserted number of twisting turns exceeded a certain critical value, and the coils were formed sequentially along the axial direction and compactly arranged, leading to the formation of a continuous and free-standing hierarchically arranged helical fiber (HHF). Upon coming into contact with a droplet of polar solvents including ethanol, acetone, toluene and dichloromethane, HHFs could produce reversibly contractive and rotary actuations (Fig. 6b). HHFs exhibited a fast response (0.5 s) because their gap structures enabled efficient infiltration of solvents via capillary force and the generated contractive stress (1.5 Mpa) was dependent on the helical angle (32°) of the primary fibers. By weaving HHFs into a flexible and strong textile, it could be used to lift a copper ball 4.5 mm within milliseconds when spraying with ethanol. Especially, the power output of 49 W kg^{-1} was generated by the smart textile during the initial 50 ms. Different from the pure CNT based artificial muscles, Mu et al. proposed sheath-run artificial muscles (SRAMs) with the CNT as the inner core and the polymer as the outer wrapping [129]. As shown in Fig. 6c, the fabrication of SRAMs was achieved by drawing a vertically suspended, torsionally tethered twisted CNT yarn through a large droplet of polymer solution and the desired sheath thickness of dried polymer was developed by repeating the process for multiple times. The solvent used was selected to furnish a sharp interface between sheath and core and prevent polymer from infiltrating into the twist-densified core yarn. As illustrated in Fig. 6d, there were three types of muscles including pristine yarns, hybrid yarn artificial muscles (HYAMs) that was made by inserting twisting and coiling into a PU-filled CNT yarn, SRAMs with PU as the wrapping and pristine CNT yarns. Among them, SRAMs exhibited highest tensile stroke when they were electrothermally driven, indicating the performance advantages of sheath-run muscles.

Supercapacitors

Lightweight and flexible electrochemical energy-storage devices are essential components to power wearable electronics. Over the past few years, research on fiber-based wearable supercapacitors has exhibited rapid growth [130]. A supercapacitor is an electrochemical cell in which energy is stored in the form of pseudocapacitance or electrical double-layer capacitance with higher power density than batteries and higher energy density than electrolytic capacitors. In general, conductive fibers are not electrochemically reactive and cannot be recognized as active materials. Instead, conductive yarns and fabrics have been used as soft current collectors for constructing supercapacitors. As shown in Fig. 7a, Liu et al. reported the fabrication of graphene-metallic yarn composite electrodes [131]. In the fabrication process, Nicotian yarns were coated with rGO flakes by electrodeposition to form rGO/Ni-cotton hybrid composite electrode, and

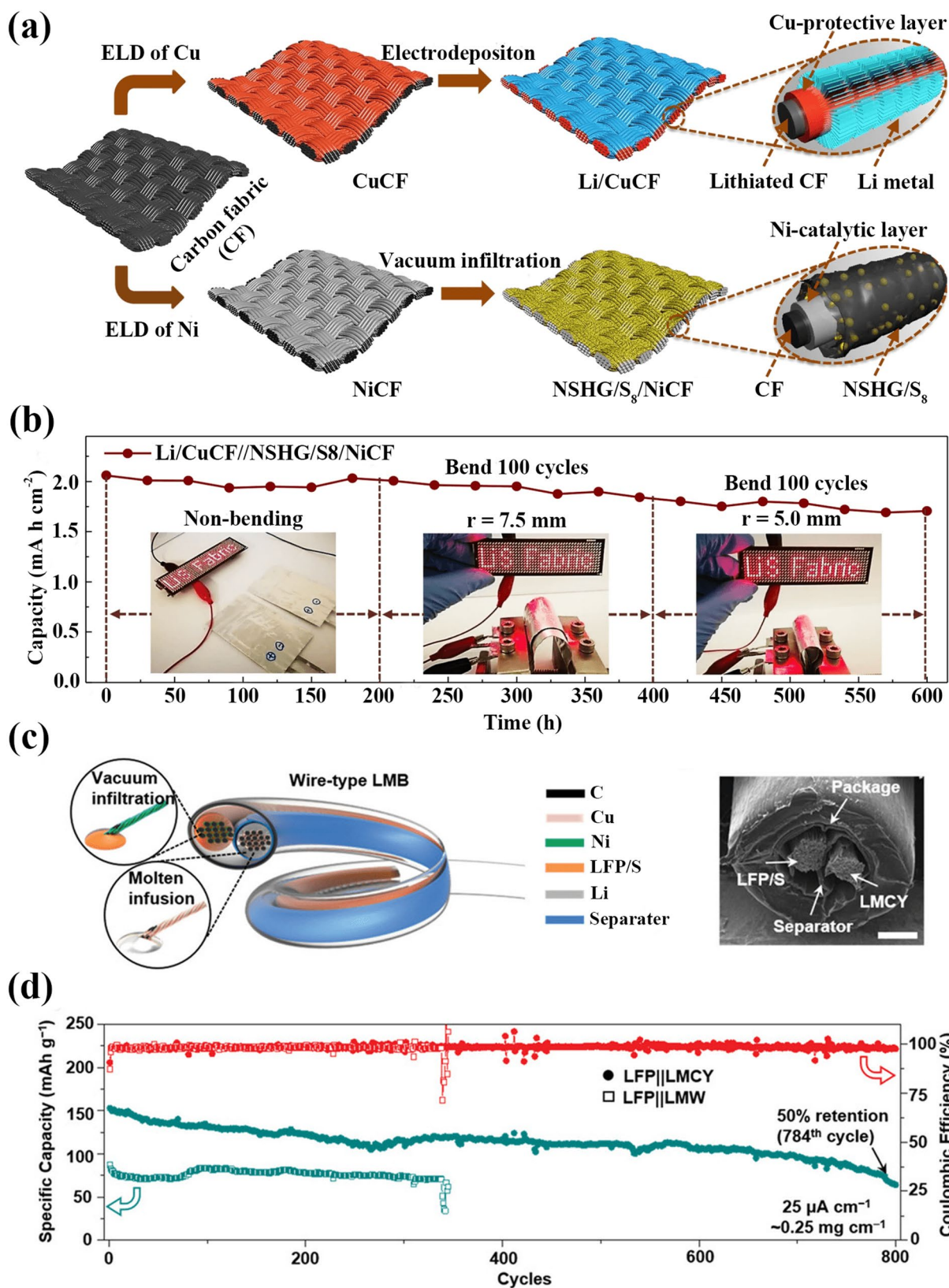


Fig. 8 **a** Schematic illustration of the fabrication process for the electrodes. **b** Areal capacity of fabric-based Li–S battery when powering the LED screen for 600 h under bending. **a, b** Reproduced with permission from Ref. [134], Copyright 2018, Springer Nature. **c**

Schematic diagram and SEM image of the wire-type Li–S battery. **d** Cycling performance of LFP||LMCY battery. **d** Reproduced with permission from Ref. [135], Copyright 2021, Wiley-VCH

gel-like polyvinyl alcohol/LiCl electrolyte were employed to fabricate solid-state supercapacitor yarns. These supercapacitors could be used as weft and warp yarns to form a woven fabric by weaving them with pristine cotton yarns (Fig. 7b). Due to the hierarchical structures and the large surface area of Ni-cotton yarns, the rGO flakes were effectively absorbed and held, leading to the high-speed electrical and ionic transportation in the charge/discharge process. As a result, the volumetric energy density and the power density of such supercapacitors were 6.1 mW h cm^{-3} and $1400 \text{ mW h cm}^{-3}$, respectively (Fig. 7c). Moreover, the coulombic efficiency of yarn-based supercapacitors was $\approx 99\%$ and over 80% of the initial capacitance remained after 10,000 charge/discharge cycles. The concept was further extended to fabrics in order to realize larger energy. As shown in Fig. 7d, Yang et al. fabricated composite fabric electrodes by using MWCNT, rGO and metallic textiles [132]. In detail, aqueous solutions of MWCNTs and rGOs were vacuum filtrated into Ni-cotton fabric, in which the 1D MWCNTs and 2D rGOs played the role of a stable scaffold in the filtration process to yield ultrathick ($400 \mu\text{m}$) hierarchically porous carbon film. For the assembly of the fabric-based supercapacitor, one piece of pristine cotton fabric was sandwiched by two symmetrical composite fabric electrodes in LiCl aqueous solution. This supercapacitor fabric device could be sewn into a lab coat to power the light-emitting diode (LED) (Fig. 7e). The areal capacitance of 2.7 F cm^{-2} at 20 mA cm^{-2} of such device was achieved when the number of MWCNT/rGO bilayer was ten (Fig. 7f). In addition, as-made fabric supercapacitors exhibited a 118% retention after 10,000 charge/discharge cycles and an unobservable performance deterioration after 10,000 bending cycles at a radius of 5 mm.

Batteries

Compared with supercapacitors, batteries generally have a higher energy density. Especially, fiber-based lithium-based batteries enable the seamless implementation of power supply to flexible wearable electronics because of their long cyclic life span, high electrochemical window, good coulombic efficiency and exceptional energy density [133]. It is noted that metal-coated carbon fibers can be used as the current collector to effectively enhance the electrochemical stability and the flexibility of both lithium (Li) and sulfur (S) electrodes. For example, Chang et al. demonstrated that stable fabric-based lithium-sulfur full batteries with only 100% oversized lithium [134]. As shown in Fig. 8a, Cu and Ni nanoparticles were firstly deposited on two carbon fabrics (CFs) via ELD, respectively. Afterwards, the Li metal was electrochemically plated on CuCF to form Li/CuCF anode and a slurry mixture containing nitrogen and sulfur heavily doped graphene (NSHG), carbon black and a S_8 in N-methyl-2-pyrrolidone

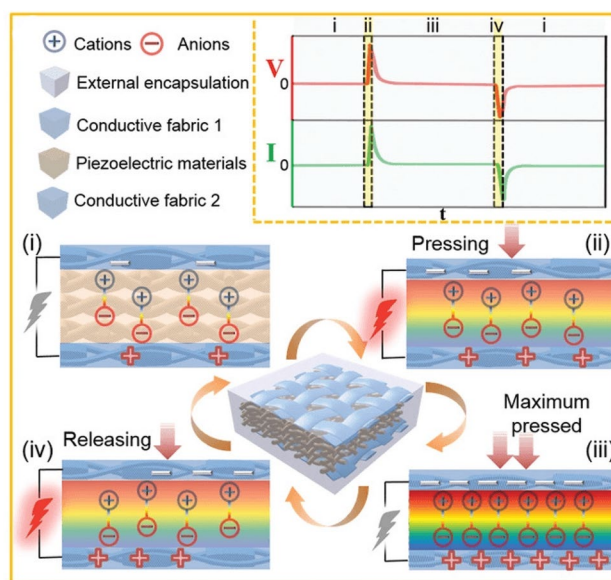


Fig. 9 Charge generation and transfer mechanisms of textile-based piezoelectric nanogenerators with four basic working modes, including the following: (i) original state, (ii) approaching to each other, (iii) fully contacted state and (iv) separating from each other; reproduced with permission from Ref. [148], Copyright 2019, Wiley-VCH

(NMP) was doctor-blade coated on NiCF to develop NSHG/ S_8 /NiCF cathode. Finally, the flexible Li-S full battery was assembled with two pieces of fabric electrodes, together with a microporous polypropylene membrane as the separator, ether-based electrolyte and aluminum (Al) plastic foil as the cell encapsulant. Importantly, the remarkably coulombic efficiency of $> 99.89\%$ for the Li anode and $> 99.82\%$ for the S cathode over 400 half-cell charge-discharge cycles were achieved because these metallic CFs with mechanical flexibility reduced local current density of the electrodes and stabilized the electrode materials. As-prepared batteries showed good cell energy density (288 W h kg^{-1} and 360 W h L^{-1}), high area capacity (3 mA h cm^{-2}), excellent bending stability at a small radius of curvature ($< 1 \text{ mm}$) and remarkable cycling stability (260 cycles). Therefore, such battery devices could be used to power the LED screen with stable brightness under bending for tens of minutes (Fig. 8b). Apart from fabric-based Li-S batteries, wire-type Li-S batteries that consist of a pair of fibrous Li anode and S cathode with paralleled, twisted, coaxial alignment have also been extensively studied due to their omnidirectional flexibility offered by the wire shape and the easy integration into wearable formats via weaving, knitting and braiding. For instance, Gao et al. reported the fabrication of high-energy and stable wire-type Li-metal batteries with flexible Li-metal composite yarns (LMCYs) that were designed via a fast capillary filling of molten Li into Cu-coated carbon

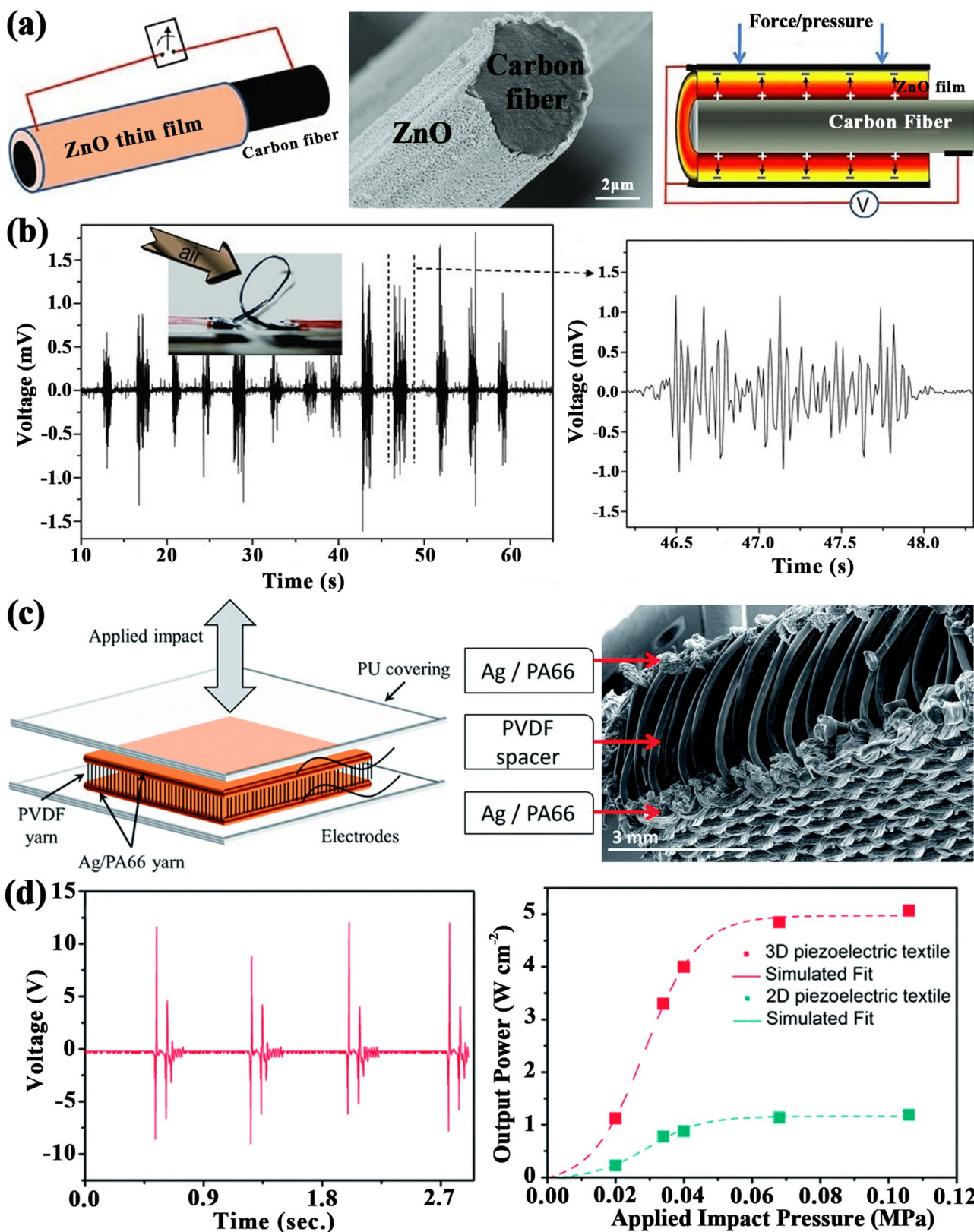


Fig. 10 **a** Schematic illustration of a fiber-based FNG and SEM image of the ZnO-coated carbon fiber. **b** Performance of the FNG consisting of a single fiber when being driven by air flow. **a**, **b** Reproduced with permission from Ref. [153], Copyright 2010, Wiley-VCH. **c** Sche-

matic diagram of the packaged 3D FNG and SEM image of the 3D fabric. **d** Performance of the 3D FNG when being driven by pressure. **c**, **d** Reproduced with permission from Ref. [154], Copyright 2014, Royal Society of Chemistry

yarn [135]. Benefitting from the good lithiophilicity of Cu coatings and the unique structure of carbon yarns, LMCYs possessed much higher electrochemical cyclic stability, mechanical strength, flexibility and durability than Li-metal wires (LMWs). As shown in Fig. 8c, LMCY was used as the anode and lithium-iron phosphate (LFP) or S slurry was dip-coated onto the Ni-deposited carbon yarn, followed by vacuum filtration to allow the sufficient penetration of active materials into the internal space of the yarn for the formation of the yarn-like cathode. The cathode and the anode were aligned in parallel, electrically isolated by a polypropylene separator and encapsulated in a polyolefin tune to form a foldable LFP||Li full cell. As-fabricated batteries showed a high energy density over 290 Wh L⁻¹ and a long lifetime over 800 cycles with a capacity retention of over 50% after 750 charge/discharge cycles (Fig. 8d).

Piezoelectric Fibers for Wearable Electronics

Besides conductive fibers, piezoelectric fibers are also very important for the construction of textile-based wearable electronics. These fibers are capable of generating electricity and thus, their applications are mainly in the flexible nanogenerator (FNG) devices [136]. Nanogenerators with piezoelectric effect provide the ability to convert the stress inside the material into electricity, while textiles endow the fiber-enabled wearable electronic with versatile flexible design carrier and extensive wearable application platform for their development [137]. In this section, material selections, fabrication techniques, structural designs, working principles and potential applications of piezoelectric fiber materials will be discussed.

Piezoelectric Materials

Many piezoelectric materials have been developed since the discovery of piezoelectricity that means stress-induced electricity and representative piezoelectric materials can be divided into piezoceramics and piezopolymers. Piezoceramics refer to piezoelectric class of inorganic materials, such as semiconducting zinc oxide (ZnO) [138], lead-based zirconate titanate (PZT) [139] and lead-free barium titanate (BaTiO₃) [140]. Piezoceramics are chemically inert, mechanically strong and immune to humidity, exhibiting high piezoelectric coefficient and electrochemical conversion efficiency [141]. However, their applications in flexible devices are limited by the intrinsic rigid nature. Piezopolymers, or organic piezoelectric materials, mainly include polyamide 11 (PA-11) [142], polypropylene (PP) [143], poly(vinylidene fluoride) (PVDF) [144] and poly(vinylidene

fluoride-*co*-tri-fluoroethylene) (PVDF-TrFE) [145]. Among them, PVDF is a semicrystalline polymer with five different crystal phases (α , β , γ , δ and ϵ), and the β phase is very important due to high piezoelectric sensitivity and exhibition of large polarization. Importantly, PVDF must be processed in such a way that it crystallizes in its β -phase for being used as a piezoelectric material [146]. To obtain a higher percentage of β phase in PVDF, various methods such as thermal drawing, in-situ poling and high electric field have been proposed. The high piezoelectric activity and availability as flexible nanofiber structures make PVDF premise potential applicability in diverse fields of technology. Compared with PVDF, PVDF-TrFE has another advantage owing to its adequately large electromechanical coupling coefficient and ferroelectricity with definite Curie transition temperature [147]. In general, PVDF and PVDF-TrFE are the most widely used in piezoelectric textiles due to their good structural flexibility, high mechanical strength, excellent chemical resistance, ease of processing and superior biocompatibility. Nevertheless, due to the much smaller piezoelectric charge constants of piezopolymers than those of piezoceramics, the practical use of piezopolymers in energy harvesting is hugely limited. Therefore, electrical poling in which mechanical stretching processes need to align the dipole of the polarization structures is required for achieving good performance.

Piezoelectric Mechanism

Metal–insulator–metal structure, made of insulating piezoelectric materials as the middle layer and two metal electrodes as the top and bottom conducting faces, was usually used for the establishment of piezoelectric nanogenerators. In Fig. 9, a whole process of an electrical generation and its corresponding output characteristics of a textile-based piezoelectric nanogenerators during one pressing and releasing movement is demonstrated [148]. At the original state, the charge centers of the cations and anions coincide with one another and there is no polarization inside the piezoelectric material. Once the nanogenerator is subjected to the pressing force, a negative strain and decreased volume are produced by the deformation of the piezofabric, causing the formation of a piezopotential between the electrodes because the charge centers separate to develop electrical dipoles and electric dipole moments change. By connecting the electrodes with an external circuit, the electrons will be driven by the piezopotential to flow through the external load in order to partially screen the piezopotential and accomplish a new equilibrium state. Therefore, the electricity is generated. When two fabric electrodes are fully contacted, the maximized press state is fulfilled and the polarization density becomes highest. As the releasing of the external force is made, the charge induced by the strain releasing in the short-circuit condition is rebalanced by the flowing back of

electrons. Based on this, a constant stream of pulse current will flow through the external load if applying a reciprocating straining phenomenon continuously changes the piezopotential. Especially, the output voltage and current of piezoelectric nanogenerators reverse their signals when the measurement system is reversely connected.

Piezoelectric Textiles

For piezoelectric nanogenerators, material selections, structural designs and potential performance are the most important aspects. For textile-based piezoelectric nanogenerators, the flexibility and wearability should be also taken into considerations. Recently, the design of piezoelectric textiles with the purpose of improving electrochemical conversion efficiency, enhancing wearable functionality and expanding application scopes has been comprehensively studied by many researchers [149–152]. As shown in Fig. 10a, Li et al. reported the FNG based on a single fiber that was the smallest structure unit of textile materials [153]. In the fabrication process, a radical textured ZnO thin film with the thickness of ca. 250 nm and the normal direction along [0001] composed of nearly parallel aligned ZnO nanorods was cylindrically covered on the surface of a carbon fiber via physical vapor deposition. From the SEM image, it could be clearly seen that ZnO nanorods were densely packed on the hexagonal flat tops of carbon fibers. Importantly, the textured film could be used as flexible nanogenerators to generate electricity through air flow. As illustrated in Fig. 10b, when a gentle exhalation blew onto the fiber-based nanogenerator, the shape and vibrate of FNGs were changed by the blowing wind, leading to an electric output. As a result, the average output voltage was 1.5 mV. However, because of limited fiber number and small active area, the piezoelectric output of single fiber-based FNGs is relatively low. Accordingly, fabric-based FNGs with textile forming structures produced by combining multiple piezoelectric fibers into 3D fabrics are usually used to boost the overall piezoelectric output. As demonstrated in Fig. 10c, Soin et al. fabricated all-polymeric fiber-based 3D structure piezoelectric nanogenerators consisting of high β -phase (80%) PVDF monofilaments as the spacer yarn interconnected between Ag-coated PA-66 yarns as the metal electrodes [154]. Due to the unique textile structure, the peak voltage of 3D piezofabrics was found to be 14 V at an applied pressure of 0.106 MPa and the output power density of 3D FNGs was nearly five times higher than that of 2D FNGs with a maximum power density of $5.10 \mu\text{W cm}^{-2}$, as shown in Fig. 10d.

Summary and Perspective

In summary, the recent process of two main fiber materials including conductive and piezoelectric fibers for wearable electronics has been systematically reviewed. For conductive fibers, conductive materials (i.e., metals, conductive polymers, carbon, liquid electrodes and MXene) and fabrication techniques (i.e., coating, fiber making and structural transformation) for the formation of conductive fibers are summarized, while their four representative applications in wearable electronics such as sensors, artificial muscles, supercapacitors and batteries are highlighted. For piezoelectric fibers, piezoelectric materials (i.e., piezoceramics and piezopolymers), working mechanisms and their application in textile-based piezoelectric nanogenerators are discussed.

First, in comparison to conventional bulk electronic devices, performances of electronic textiles are relatively poor. Electrical conductivities of conductive fibers are much lower than those of thin-film electrodes because the diameters of them are very small. Despite the fact that some studies such as designing device structures or providing high-quality conductive materials have been conducted to promote the performances of fiber-based electronics, a balance between electrical and mechanical properties of electronic textiles needs to be realized. Moreover, mechanical stability of fibrous electronics under different deformations such as bending, washing and twisting needs has not been really achieved. For example, the coating layer of conductive materials on the surface of fibers is very easy to peel off during the repeated washing of conductive fibers. Thus, it is necessary to maintain the structural integrity of electronic textiles while constructing the desired electrical performance.

Second, in order to commercialize fiber-shaped wearable electronics, it is crucial to ensure that the requirements of practical applications can be satisfied by the performances of fiber-enabled electronic devices while the technologies to produce flexible and breathable wearable electronics on a large scale is efficient. Up to now, weaving by hand at the laboratory scale is still the main method to transform smart fibers into electronic textiles. To achieve the advancement of large-scale fabrication, developing new machine weaving technologies with high efficiency to yield textile-based electronic devices is essential. Furthermore, because of the interference between different functions, multi-functions are difficult to be integrated into electronic textiles. In addition, besides the above-mentioned functions including sensing, actuating, energy storage and energy harvesting, the integration of computing parts, personal data security services and information acquisition functions has not been explored.

Third, there is a lack of uniform technical and testing standards and thus, the performances of electronic textiles

are difficult to be compared. In different reports, parameters for flexible electronics are calculated by various methods, leading to the fact that it is difficult to compare fiber-shaped wearable electronics with different functions or even the same function. Additionally, although flexibility is an important property to sustain bending, stretching and twisting of electronic devices, the evaluation standards are not consistent. In the future, the joint efforts of scientists in various disciplines will be required for the standardization of smart textile wearables and the commercial potentials of smart fiber products will be increased by such interdisciplinary cooperation, resulting in the acceleration of applications of flexible and wearable electronics in digitalization, intelligence and human health.

In summary, the current research of fiber materials has made great development and tremendous applications prospects in the field of fiber-based wearable electronics. In future, electronic textiles with integrated features of unique structures and various functions are expected to not only meet the needs of wears daily but also serve the emerging domains of health diagnosis, human–machine interactions and artificial intelligence, which will innovate the way of people's lives. Although this field faces substantial challenges, functional fiber materials with unprecedented properties will continue to play a decisive role in the development of wearable electronics with the continuous efforts of researchers from different areas.

Acknowledgements This work was supported by the Fundamental Research Funds for the Central Universities (2232022D-15).

Declarations

Conflict of interest The authors declare no conflicts of interest.

Open Access This article is licensed under a Creative Commons Attribution 4.0 International License, which permits use, sharing, adaptation, distribution and reproduction in any medium or format, as long as you give appropriate credit to the original author(s) and the source, provide a link to the Creative Commons licence, and indicate if changes were made. The images or other third party material in this article are included in the article's Creative Commons licence, unless indicated otherwise in a credit line to the material. If material is not included in the article's Creative Commons licence and your intended use is not permitted by statutory regulation or exceeds the permitted use, you will need to obtain permission directly from the copyright holder. To view a copy of this licence, visit <http://creativecommons.org/licenses/by/4.0/>.

References

- Wang W, Yu AF, Zhai JY, Wang ZL. Recent progress of functional fiber and textile triboelectric nanogenerators: towards electricity power generation and intelligent sensing. *Adv Fiber Mater* **2021**;3:394.
- Xue JJ, Xie JW, Liu WY, Xia YN. Electrospun nanofibers: new concepts, materials, and applications. *Acc Chem Res* **1976**;2017:50.
- Chen GR, Li YZ, Bick M, Chen J. Smart textiles for electricity generation. *Chem Rev* **2020**;120:3668.
- Qi XJ, Zhao HT, Wang LH, Sun FQ, Ye XR, Zhang XJ, Tian MW, Qu LJ. Underwater sensing and warming E-textiles with reversible liquid metal electronics. *Chem Eng J* **2022**;437:135382.
- Chen LM, Lu MY, Wang YQ, Huang YH, Zhu S, Tang JW, Zhu C, Liu XQ, Yin WL. Whole system design of a wearable magnetic induction sensor for physical rehabilitation. *Adv Intell Syst* **2019**;1:1970020.
- Zhang YY, Liu SJ, Yan JH, Zhang XH, Xia SH, Zhao Y, Yu JY, Ding B. Superior flexibility in oxide ceramic crystal nanofibers. *Adv Mater* **2021**;33:2105011.
- Fang YS, Chen GR, Bick M, Chen J. Smart textiles for personalized thermoregulation. *Chem Soc Rev* **2021**;50:9357.
- Chen GR, Fang YS, Zhao X, Tat T, Chen J. Textiles for learning tactile interactions. *Nat Electron* **2021**;4:175.
- Libanori A, Chen GR, Zhao X, Zhou YH, Chen J. Smart textiles for personalized healthcare. *Nat Electron* **2022**;5:142.
- Chen GR, Xiao X, Zhao X, Tat T, Bick M, Chen J. Electronic textiles for wearable point-of-care systems. *Chem Rev* **2022**;122:3259.
- Guo Y, Liu H, Wang DD, Bahy Z, Althakafy J, Dief H, Guo ZH, Xu B, Liu CT, Shen CY. Engineering hierarchical heterostructure material based on metal-organic frameworks and cotton fiber for high-efficient microwave absorber. *Nano Res* **2022**;15:6841.
- Zeng W, Shu L, Li Q, Chen S, Wang F, Tao XM. Fiber-based wearable electronics: a review of materials, fabrication, devices, and applications. *Adv Mater* **2014**;26:5310.
- Fukuda K, Someya T. Recent progress in the development of printed thin-film transistors and circuits with high-resolution printing technology. *Adv Mater* **2017**;29:1602736.
- Hirsch A, Dejace L, Michaud H, Lacour S. Harnessing the rheological properties of liquid metals to shape soft electronic conductors for wearable applications. *Acc Chem Res* **2019**;52:534.
- Sun FQ, Tian MW, Sun XT, Xu TL, Liu XQ, Zhu SF, Zhang XJ, Qu LJ. Stretchable conductive fibers of ultrahigh tensile strain and stable conductance enabled by a worm-shaped graphene microlayer. *Nano Lett* **2019**;19:6592.
- Li LP, Wang HZ. Unipolar-stroke electrochemical artificial muscles. *Adv Fiber Mater* **2021**;3:147.
- Islam N, Ali A, Collie S. Textile sensors for wearable applications: a comprehensive review. *Cellulose* **2020**;27:6103.
- Zeng L, Liu XQ, Chen XG, Soutis C. π – π interaction between carbon fibre and epoxy resin for interface improvement in composites. *Compos B Eng* **2021**;220:108983.
- Jiang ZW, Karan S, Livingston A. Water transport through ultrathin polyamide nanofilms used for reverse osmosis. *Adv Mater* **2018**;30:1705973.
- Ma LY, Nie Y, Liu YR, Huo F, Bai L, Li Q, Zhang SJ. Preparation of core/shell electrically conductive fibers by efficient coating carbon nanotubes on polyester. *Adv Fiber Mater* **2021**;3:180.
- Li YH, Zhou B, Zheng GQ, Liu XH, Li TX, Yan C, Cheng CB, Dai K, Liu CT, Shen CY, Guo ZH. Continuously prepared highly conductive and stretchable SWNT/MWNT synergistically composited electrospun thermoplastic polyurethane yarns for wearable sensing. *J Mater Chem C* **2018**;6:2258.
- Deng W, Sun YJ, Yao XX, Subramanian K, Ling C, Wang HB, Chopra S, Xu B, Wang JX, Chen JF, Wang D, Amancio H, Pramana S, Ye RQ, Wang S. Masks for COVID-19. *Adv Sci* **2022**;9:2102189.
- Liu XH, Miao JL, Fan Q, Zhang WX, Zuo XW, Tian MW, Zhu SF, Zhang XJ, Qu LJ. Recent progress on smart fiber and textile

- based wearable strain sensors: materials, fabrications and applications. *Adv Fiber Mater* **2022**;4:361.
24. Zeng MX, Zavanelli D, Chen JH, Javash M, Du YP, LeBlanc S, Snyder J, Zhang YL. Printing thermoelectric inks toward next-generation energy and thermal devices. *Chem Soc Rev* **2022**;51:485.
 25. Kim M, Fan JT. Piezoelectric properties of three types of PVDF and ZnO nanofibrous composites. *Adv Fiber Mater* **2021**;3:160.
 26. Su M, Song YL. Printable smart materials and devices: strategies and applications. *Chem Rev* **2022**;122:5144.
 27. Zhou ZH, Chen K, Li XS, Zhang SL, Wu YF, Zhou YH, Meng KY, Sun CC, He Q, Fan WJ, Fan ED, Lin ZW, Tan XL, Deng WL, Yang J, Chen J. Sign-to-speech translation using machine-learning-assisted stretchable sensor arrays. *Nat Electron* **2020**;3:571.
 28. Zhao X, Zhou YH, Xu J, Chen GR, Fang YS, Tat T, Xiao X, Song Y, Li S, Chen J. Soft fibers with magnetoelasticity for wearable electronics. *Nat Commun* **2021**;12:6755.
 29. Woo J, Lee H, Yi C, Lee J, Won C, Oh S, Jekal J, Kwon C, Lee S, Song J, Choi B, Jang K, Lee T. Ultrastretchable helical conductive fibers using percolated Ag nanoparticle networks encapsulated by elastic polymers with high durability in omnidirectional deformations for wearable electronics. *Adv Funct Mater* **2020**;30:1910026.
 30. Liu ZK, Zhu TX, Wang JR, Zheng ZJ, Li Y, Li JS, Lai YK. Functionalized fiber-based strain sensors: pathway to next-generation wearable electronics. *Nano-Micro Lett* **2022**;14:61.
 31. Qian F, Lan PC, Freyman M, Chen W, Kou TY, Olson T, Zhu C, Worsley M, Duoss E, Spadaccini C, Baumann T, Han Y. Ultralight conductive silver nanowire aerogels. *Nano Lett* **2017**;17:7171.
 32. Zadeh K, Rahim A, Tang JB. Low melting temperature liquid metals and their impacts on physical chemistry. *Acc Mater Res* **2021**;2:577.
 33. Shi Y, Peng LL, Ding Y, Zhao Y, Yu GH. Nanostructured conductive polymers for advanced energy storage. *Chem Soc Rev* **2015**;44:6684.
 34. Hodge S, Bayazit M, Coleman K, Shaffer M. Unweaving the rainbow: a review of the relationship between single-walled carbon nanotube molecular structures and their chemical reactivity. *Chem Soc Rev* **2012**;41:4409.
 35. Zhao MQ, Xie XQ, Ren C, Makaryan T, Anasori B, Wang GX, Gogotsi Y. Hollow MXene spheres and 3D macroporous mxene frameworks for Na-Ion storage. *Adv Mater* **2017**;29:1702410.
 36. Karim N, Afroj S, Tan SR, He P, Fernando A, Carr C, Novoselov K. Scalable production of graphene-based wearable E-textiles. *ACS Nano* **2017**;11:12266.
 37. Qu YP, Dang T, Page A, Yan W, Gupta T, Rotaru G, Rossi R, Favrod V, Bartolomei N, Sorin F. Superelastic multimaterial electronic and photonic fibers and devices via thermal drawing. *Adv Mater* **2018**;30:1707251.
 38. Liu ZK, Li ZH, Zhai H, Jin L, Chen KL, Yi YPQ, Gao Y, Xu LL, Zheng Y, Yao SR, Liu ZC, Li G, Song QW, Yue PF, Xie SQ, Li Y, Zheng ZJ. A highly sensitive stretchable strain sensor based on multi-functionalized fabric for respiration monitoring and identification. *Chem Eng J* **2021**;426:130869.
 39. Kim S, Haines C, Li N, Kim K, Mun T, Choi C, Di JT, Oh Y, Oviedo J, Bykova J, Fang SL, Jiang N, Liu ZF, Wang R, Kumar P, Qiao R, Priya S, Cho K, Kim M, Lucas M, Drummy L, Maruyama B, Lee D, Lepró X, Gao E, Albarq D, Robles R, Kim S, Baughman R. Harvesting electrical energy from carbon nanotube yarn twist. *Science* **2017**;357:773.
 40. Davies A, Audette P, Farrow B, Hassan F, Chen ZW, Choi J, Yu AP. Graphene-based flexible supercapacitors: pulse-electropolymerization of polypyrrole on free-standing graphene films. *J Phys Chem C* **2011**;115:17612.
 41. Lin HJ, Weng W, Ren J, Qiu LB, Zhang ZT, Chen PN, Chen XL, Deng J, Wang YG, Peng HS. Twisted aligned carbon nanotube/silicon composite fiber anode for flexible wire-shaped lithium-ion battery. *Adv Mater* **2014**;26:1217.
 42. Eom J, Jaisutti R, Lee H, Lee W, Heo J, Lee J, Park S, Kim Y. Highly sensitive textile strain sensors and wireless user-interface devices using all-polymeric conducting fibers. *ACS Appl Mater Interfaces* **2017**;9:10190.
 43. Zhang FZ, Chen J, Yang JP. Fiber materials for electrocatalysis applications. *Adv Fiber Mater* **2022**;4:720.
 44. Chen S, Lou Z, Chen D, Jiang K, Shen GZ. Polymer-enhanced highly stretchable conductive fiber strain sensor used for electronic data gloves. *Adv Mater Technol* **2016**;1:1600136.
 45. Wang DR, Zhang YK, Lu X, Ma ZJ, Xie C, Zheng ZJ. Chemical formation of soft metal electrodes for flexible and wearable electronics. *Chem Soc Rev* **2018**;47:4611.
 46. Wang T, Bao YW, Zhuang MD, Li JC, Chen JC, Xu HX. Nanoscale engineering of conducting polymers for emerging applications in soft electronics. *Nano Res* **2021**;14:3112.
 47. Lin S, Liu JC, Li WZ, Wang D, Huang Y, Jia C, Li ZW, Murtaza M, Wang HY, Song JN, Liu ZL, Huang K, Zu D, Lei M, Hong B, Wu H. A flexible, robust, and gel-free electroencephalogram electrode for noninvasive brain-computer interfaces. *Nano Lett* **2019**;19:6853.
 48. Tyagi P, Postetter D, Saragnese D, Randall C, Mirski M, Gracias D. Patternable nanowire sensors for electrochemical recording of dopamine. *Anal Chem* **2009**;81:9979.
 49. Zhao SF, Meng XY, Liu L, Bo WJ, Xia ML, Zhang RL, Cao DX, Ahn J. Polypyrrole-coated copper nanowire-threaded silver nanoflowers for wearable strain sensors with high sensing performance. *Chem Eng J* **2021**;417:127966.
 50. Chen MX, Wang Z, Li KW, Wang XD, Wei L. Elastic and stretchable functional fibers: a review of materials, fabrication methods, and applications. *Adv Fiber Mater* **2021**;3:1.
 51. Kim C, Kim M. Intrinsically conducting polymer (ICP) coated aramid fiber reinforced composites for broadband radar absorbing structures (RAS). *Compos Sci Technol* **2021**;211:108827.
 52. Bag A, Lee E. Recent advancements in development of wearable gas sensors. *Adv Mater Technol* **2021**;6:2000883.
 53. Chen HW, Li C. PEDOT: fundamentals and its nanocomposites for energy storage. *Chin J Polym Sci* **2020**;38:435.
 54. Yuan DM, Li B, Cheng JL, Guan Q, Wang ZP, Ni W, Li C, Liu H, Wang B. Twisted yarns for fiber-shaped supercapacitors based on wet-spun PEDOT:PSS fibers from aqueous coagulation. *J Mater Chem A* **2016**;4:11616.
 55. Yi M, Shen ZG. A review on mechanical exfoliation for the scalable production of graphene. *J Mater Chem A* **2015**;3:11700.
 56. Lee J, Zambrano B, Woo J, Yoon K, Lee T. Recent advances in 1D stretchable electrodes and devices for textile and wearable electronics: materials, fabrications, and applications. *Adv Mater* **2020**;32:1902532.
 57. Zhao D, Liu R, Luo C, Guo Y, Hou CY, Zhang QH, Li YG, Jia W, Wang HZ. Dielectrophoretic assembly of carbon nanotube chains in aqueous solution. *Adv Fiber Mater* **2021**;3:312.
 58. Volder M, Tawfik S, Baughman R, Hart J. Carbon nanotubes: present and future commercial applications. *Science* **2013**;339:535.
 59. Olabi A, Abdelkareem M, Wilberforce T, Sayed E. Application of graphene in energy storage device—a review. *Renew Sust Energy Rev* **2021**;135:110026.
 60. Kim J, Chang W, Kim D, Yang J, Han J, Lee G, Kim J, Seol S. 3D printing of reduced graphene oxide nanowires. *Adv Mater* **2015**;27:157.
 61. Wang Q, Yu Y, Liu J. Preparations, characteristics and applications of the functional liquid metal materials. *Adv Eng Mater* **2018**;20:1700781.

62. Zhang MK, Yao SY, Rao W, Liu J. Transformable soft liquid metal micro/nanomaterials. *Mater Sci Eng R Rep* **2019**;138:1.
63. He JF, Liang ST, Li FJ, Yang QB, Huang MJ, He Y, Fan XN, Wu ML. Recent development in liquid metal materials. *ChemistryOpen* **2021**;10:360.
64. Chen S, Wang HZ, Zhao RQ, Rao W, Liu J. Liquid metal composites. *Matter* **2020**;2:1446.
65. Naguib M, Kurtoglu M, Presser V, Lu J, Niu JJ, Heon M, Hultman L, Gogotsi Y, Barsoum M. Two-dimensional nanocrystals produced by exfoliation of Ti_3AlC_2 . *Adv Mater* **2011**;23:4248.
66. Jin C, Bai ZQ. MXene-based textile sensors for wearable applications. *ACS Sens* **2022**;7:929.
67. Ahmed A, Hossain M, Adak B, Mukhopadhyay S. Recent advances in 2D MXene integrated smart-textile interfaces for multifunctional applications. *Chem Mater* **2020**;32:10296.
68. VahidMohammadi A, Rosen J, Gogotsi Y. The world of two-dimensional carbides and nitrides (MXenes). *Science* **2021**;372:eabf1581.
69. Ma C, Ma MG, Si CL, Ji XX, Wan PB. Flexible MXene-based composites for wearable devices. *Adv Funct Mater* **2021**;31:2009524.
70. Zhang JZ, Kong N, Uzun S, Levitt A, Seyedin S, Lynch P, Qin S, Han MK, Yang WR, Liu JQ, Wang XG, Gogotsi Y, Razal J. Scalable manufacturing of free-standing, strong Ti_3C_2Tx MXene films with outstanding conductivity. *Adv Mater* **2020**;32:2001093.
71. Krebs F. Fabrication and processing of polymer solar cells: a review of printing and coating techniques. *Sol Energy Mater Sol Cells* **2009**;93:394.
72. Xiang SW, Zhang NN, Fan X. From fiber to fabric: progress towards photovoltaic energy textile. *Adv Fiber Mater* **2021**;3:76.
73. Wang WS, Gan Q, Zhang YQ, Lu X, Wang HX, Zhang YK, Hu H, Chen LN, Shi LX, Wang ST, Zheng ZJ. Polymer-assisted metallization of mammalian cells. *Adv Mater* **2021**;33:2102348.
74. Arulvel S, Mallikarjuna R, Dsilva D, Akinaga T. A comprehensive review on mechanical and surface characteristics of composites reinforced with coated fibres. *Surf Interfaces* **2021**;27:101449.
75. Kim S, Gang H, Park G, Jeon H, Jeong Y. Electromagnetic interference shielding and electrothermal performance of MXene-coated cellulose hybrid papers and fabrics manufactured by a facile scalable dip-dry coating process. *Adv Eng Mater* **2021**;23:2100548.
76. Srinivasan S, Chhatre S, Mabry J, Cohen R, McKinley G. Solution spraying of poly(methyl methacrylate) blends to fabricate microtextured, superoleophobic surfaces. *Polymer* **2011**;52:3209.
77. Li DD, Lai WY, Feng F, Huang W. Post-treatment of screen-printed silver nanowire networks for highly conductive flexible transparent films. *Adv Mater Interfaces* **2021**;8:2100548.
78. Paudyal J, Wang P, Zhou FY, Liu YZ, Cai Y, Xiao Y. Platinum-nanoparticle-modified single-walled carbon nanotube-laden paper electrodes for electrocatalytic oxidation of methanol. *ACS Appl Nano Mater* **2021**;4:13798.
79. Zhu C, Chalmers E, Chen LM, Wang YQ, Xu B, Li Y, Liu XQ. A nature-inspired, flexible substrate strategy for future wearable electronics. *Small* **2019**;15:1902440.
80. Jang E, Kang T, Im H, Baek S, Kim S, Jeong D, Park Y, Kim Y. Macroscopic single-walled-carbon-nanotube fiber self-assembled by dip-coating method. *Adv Mater* **2009**;21:4357.
81. Chen GZ, Wang HM, Guo R, Duan MH, Zhang YY, Liu J. Superelastic EGaIn composite fibers sustaining 500% tensile strain with superior electrical conductivity for wearable electronics. *ACS Appl Mater Interfaces* **2020**;12:6112.
82. Li P, Zhang YK, Zheng ZJ. Polymer-assisted metal deposition (PAMD) for flexible and wearable electronics: principle, materials, printing, and devices. *Adv Mater* **2019**;31:1902987.
83. Chen LM, Lu MY, Yang HS, Avila J, Shi BW, Ren L, Wei GW, Liu XQ, Yin WL. Textile-based capacitive sensor for physical rehabilitation via surface topological modification. *ACS Nano* **2020**;14:8191.
84. Zhang YZ, Wang Y, Cheng T, Yao LQ, Li XC, Lai WY, Huang W. Printed supercapacitors: materials, printing and applications. *Chem Soc Rev* **2019**;48:3229.
85. Ma ZJ, Huang QY, Xu Q, Zhuang QN, Zhao X, Yang YH, Qiu H, Yang ZL, Wang C, Chai Y, Zheng ZJ. Permeable superelastic liquid-metal fibre mat enables biocompatible and monolithic stretchable electronics. *Nat Mater* **2021**;20:859.
86. Zhang SQ, Zhao GZ, Rao M, Schmidt R, Yu YJ. A review on modeling techniques of piezoelectric integrated plates and shells. *J Intell Mater Syst Struct* **2019**;30:1133.
87. Ma ZL, Kang SL, Ma JZ, Shao L, Wei AJ, Liang CB, Gu JW, Yang B, Dong DD, Wei LF, Ji ZY. High-performance and rapid-response electrical heaters based on ultraflexible, heat-resistant, and mechanically strong aramid nanofiber/Ag nanowire nanocomposite papers. *ACS Nano* **2019**;13:7578.
88. Xiang R, Zeng HQ, Su YQ, Gui XC, Wu TZ, Einarsson E, Maruyama S, Tang ZK. Spray coating as a simple method to prepare catalyst for growth of diameter-tunable single-walled carbon nanotubes. *Carbon* **2013**;64:537.
89. Xie XX, Huang H, Zhu J, Yu JR, Wang Y, Hu ZM. A spirally layered carbon nanotube-graphene/polyurethane composite yarn for highly sensitive and stretchable strain sensor. *Compos Part A Appl Sci Manuf* **2020**;135:105932.
90. Li XH, Zhang YY, Zhang L, Xia SH, Zhao Y, Yan JH, Yu JY, Ding B. Synthesizing superior flexible oxide perovskite ceramic nanofibers by precisely controlling crystal nucleation and growth. *Small* **2022**;18:2106500.
91. Shang LR, Yu YR, Liu YX, Chen ZY, Kong TT, Zhao YJ. Spinning and applications of bioinspired fiber systems. *ACS Nano* **2019**;13:2749.
92. Yan W, Richard I, Kurtuldu G, James N, Schiavone G, Squair J, Dang T, Gupta T, Qu YP, Cao J, Ignatans R, Lacour S, Tileli V, Courtine G, Löffler J, Sorin F. Structured nanoscale metallic glass fibres with extreme aspect ratios. *Nat Nanotechnol* **2020**;15:875.
93. Gao Y, Zhang J, Su Y, Wang H, Wang XX, Huang LP, Yu M, Ramakrishna S, Long YZ. Recent progress and challenges in solution blow spinning. *Mater Horiz* **2021**;8:426.
94. Liu SJ, Zhao Y, Li XH, Yu JY, Yan JH, Ding B. Solid-state lithium metal batteries with extended cycling enabled by dynamic adaptive solid-state interfaces. *Adv Mater* **2021**;33:2008084.
95. Javed K, Krumme A, Viirsalu M, Krasnou I, Plamus T, Vassiljeva V, Tarasova E, Savest N, Mere A, Mikli V, Danilson M, Kaljuvee T, Lange S, Yuan QC, Topham P, Chen CM. A method for producing conductive graphene biopolymer nanofibrous fabrics by exploitation of an ionic liquid dispersant in electrospinning. *Carbon* **2018**;140:148.
96. Zhang J, Wang Z, Wang ZX, Wei L. Advanced multi-material optoelectronic fibers: a review. *J Lightw Technol* **2021**;39:3836.
97. Marion J, Gupta N, Cheung H, Monir K, Anikeeva P, Fink Y. Thermally drawn highly conductive fibers with controlled elasticity. *Adv Mater* **2022**;34:2201081.
98. Keneth E, Kamyshny A, Totaro M, Beccai L, Magdassi S. 3D printing materials for soft robotics. *Adv Mater* **2021**;33:2003387.

99. Cao WT, Ma C, Mao DS, Zhang J, Ma MG, Chen F. MXene-reinforced cellulose nanofibril inks for 3D-printed smart fibres and textiles. *Adv Funct Mater* **2019**;29:1905898.
100. Liu LX, Chen W, Zhang HB, Ye LX, Wang ZG, Zhang Y, Min P, Yu ZZ. Super-tough and environmentally stable aramid. Nanofiber@MXene coaxial fibers with outstanding electromagnetic interference shielding efficiency. *Nano-Micro Lett*. **2022**;14:111.
101. Tang PP, Deng ZM, Zhang Y, Liu LX, Wang ZG, Yu ZZ, Zhang HB. Tough, strong, and conductive graphene fibers by optimizing surface chemistry of graphene oxide precursor. *Adv Funct Mater* **2022**;32:2112156.
102. Cui TT, Yu JF, Li Q, Wang CF, Chen S, Li WJ, Wang GF. Large-scale fabrication of robust artificial skins from a biodegradable sealant-loaded nanofiber scaffold to skin tissue via microfluidic blow-spinning. *Adv Mater* **2020**;32:2000982.
103. Li ZW, Cui ZW, Zhao LH, Hussain N, Zhao YZ, Yang C, Jiang XY, Li L, Song JN, Zhang BP, Cheng ZK, Wu H. High-throughput production of kilogram-scale nanofibers by Kármán vortex solution blow spinning. *Sci Adv* **2022**;8:eabn3690.
104. Jordahl J, Solorio L, Sun HL, Ramcharan S, Teeple C, Haley H, Lee K, Eyster T, Luker G, Krebsbach P, Lahann J. 3D jet writing: functional microtissues based on tessellated scaffold architectures. *Adv Mater* **2018**;30:1707196.
105. Nain R, Singh D, Jassal M, Agrawal A. Zinc oxide nanorod assisted rapid single-step process for the conversion of electrospun poly(acrylonitrile) nanofibers to carbon nanofibers with a high graphitic content. *Nanoscale* **2016**;8:4360.
106. Yang L, Ji HD, Meng CZ, Li YH, Zheng GH, Chen X, Niu GY, Yan JY, Xue Y, Guo SJ, Cheng HY. Intrinsically breathable and flexible NO₂ gas sensors produced by laser direct writing of self-assembled block copolymers. *ACS Appl Mater Interfaces* **2022**;14:17818.
107. Lin X, Xia SH, Zhang L, Zhang YY, Sun SM, Chen YH, Chen S, Ding B, Yu JY, Yan JH. Fabrication of flexible mesoporous black Nb₂O₅ nanofiber films for visible-light-driven photocatalytic CO₂ reduction into CH₄. *Adv Mater* **2022**;34:2200756.
108. Yan JH, Zhang YY, Zhao Y, Song J, Xia SH, Liu SJ, Yu JY, Ding B. Transformation of oxide ceramic textiles from insulation to conduction at room temperature. *Sci Adv* **2020**;6:eaay8538.
109. Zhang MC, Wang CY, Wang HM, Jian MQ, Hao XY, Zhang YY. Carbonized cotton fabric for high-performance wearable strain sensors. *Adv Funct Mater* **2017**;27:1604795.
110. Yan JH, Dong KQ, Zhang YY, Wang X, Aboalhassan A, Yu JY, Ding B. Multifunctional flexible membranes from sponge-like porous carbon nanofibers with high conductivity. *Nat Commun* **2019**;10:5584.
111. Wan ZF, Chen X, Gu M. Laser scribed graphene for supercapacitors. *Opto-Electron Adv* **2021**;4:200079.
112. Wang HM, Wang HM, Wang YL, Su XY, Wang CY, Zhang MC, Jian MQ, Xia KL, Liang XP, Lu HJ, Li S, Zhang YY. Laser writing of janus graphene/kevlar textile for intelligent protective clothing. *ACS Nano* **2020**;14:3219.
113. Xiao RM, Yu GQ, Xu B, Wang N, Liu XQ. Fiber surface/interfacial engineering on wearable electronics. *Small* **2021**;17:2102903.
114. Heo J, Eom J, Kim Y, Park S. Recent progress of textile-based wearable electronics: a comprehensive review of materials, devices, and applications. *Small* **2018**;14:1703034.
115. Liu ZK, Zheng Y, Jin L, Chen KL, Zhai H, Huang QY, Chen ZD, Yi YYPQ, Umar M, Xu LL, Li G, Song QW, Yue PF, Li Y, Zheng ZJ. Highly breathable and stretchable strain sensors with insensitive response to pressure and bending. *Adv Funct Mater* **2021**;31:2007622.
116. Haines C, Lima M, Li N, Spinks G, Foroughi J, Madden J, Kim S, Fang SL, Andrade M, Göktepe F, Göktepe Ö, Mirvakili S, Naficy S, Lepró X, Oh J, Kozlov M, Kim S, Xu XR, Swedlove B, Wallace G, Baughman R. Artificial muscles from fishing line and sewing thread. *Science* **2014**;343:868.
117. Wang HM, Diao YF, Lu Y, Yang HR, Zhou QJ, Chruski K, Arcy J. Energy storing bricks for stationary PEDOT supercapacitors. *Nat Commun* **2020**;11:3882.
118. Zhao Y, Chen BB, Xia SH, Yu JY, Yan JH, Ding B. Selective nucleation and targeted deposition effect of lithium in a lithium-metal host anode. *J Mater Chem A* **2021**;9:5381.
119. Tan CX, Dong ZG, Li YH, Zhao HG, Huang XY, Zhou ZC, Jiang JW, Long YZ, Jiang PK, Zhang TY, Sun B. A high performance wearable strain sensor with advanced thermal management for motion monitoring. *Nat Commun* **2020**;11:3530.
120. Meng KY, Xiao X, Wei WX, Chen GR, Nashalian A, Shen S, Xiao X, Chen J. Wearable pressure sensors for pulse wave monitoring. *Adv Mater* **2022**;34:2109357.
121. Xue LL, Fan W, Yu Y, Dong K, Liu CK, Sun YL, Zhang C, Chen WC, Lei RX, Rong K, Wang Q. A novel strategy to fabricate core-sheath structure piezoelectric yarns for wearable energy harvesters. *Adv Fiber Mater* **2021**;3:239.
122. Luo JJ, Gao WC, Wang ZL. The triboelectric nanogenerator as an innovative technology toward intelligent sports. *Adv Mater* **2021**;33:2004178.
123. Ajeev A, Javaregowda B, Ali A, Modak M, Patil S, Khatua S, Ramadoss M, Kothavade P, Arulraj A. Ultrahigh sensitive carbon-based conducting rubbers for flexible and wearable human-machine intelligence sensing. *Adv Mater Technol* **2020**;5:2000690.
124. Zhu C, Li RH, Chen X, Chalmers E, Liu XT, Wang YQ, Xu B, Liu XQ. Ultraelastic yarns from curcumin-assisted ELD toward wearable human-machine interface textiles. *Adv Sci* **2020**;7:2002009.
125. Niu HS, Gao S, Yue WJ, Li Y, Zhou WJ, Liu H. Highly morphology-controllable and highly sensitive capacitive tactile sensor based on epidermis-dermis-inspired interlocked asymmetric-nanocone arrays for detection of tiny pressure. *Small* **2020**;16:1904774.
126. Atalay O, Atalay A, Gafford J, Walsh C. A highly sensitive capacitive-based soft pressure sensor based on a conductive fabric and a microporous dielectric layer. *Adv Mater Technol* **2018**;3:1700237.
127. Lima M, Li N, Andrade M, Fang SL, Oh J, Spinks G, Kozlov M, Haines C, Suh D, Foroughi J, Kim S, Chen YS, Ware T, Shin M, Machado L, Fonseca A, Madden J, Voit W, Galvão D, Baughman R. Electrically, chemically, and photonically powered torsional and tensile actuation of hybrid carbon nanotube yarn muscles. *Science* **2012**;338:928.
128. Chen PN, Xu YF, He SS, Sun XM, Pan SW, Deng J, Chen DY, Peng HS. Hierarchically arranged helical fibre actuators driven by solvents and vapours. *Nat Nanotechnol* **2015**;10:1077.
129. Mu JK, Andrade M, Fang SL, Wang XM, Gao EL, Li N, Kim S, Wang HZ, Hou CY, Zhang QH, Zhu MF, Qian D, Lu HB, Kongahage D, Talebian S, Foroughi J, Spinks G, Kim H, Ware T, Sim H, Lee D, Jang Y, Kim S, Baughman R. Sheath-run artificial muscles. *Science* **2019**;365:150.
130. Zhou Y, Wang CH, Lu W, Dai LM. Recent advances in fiber-shaped supercapacitors and lithium-ion batteries. *Adv Mater* **2020**;32:1902779.
131. Liu LB, Yu Y, Yan C, Li K, Zheng ZJ. Wearable energy-dense and power-dense supercapacitor yarns enabled by scalable graphene-metallic textile composite electrodes. *Nat Commun* **2015**;6:7260.

132. Yang Y, Huang QY, Niu LY, Wang DR, Yan C, She YY, Zheng ZJ. Waterproof, ultrahigh areal-capacitance, wearable supercapacitor fabrics. *Adv Mater* **2017**;29:1606679.
133. Zhao Y, Chen S, Guan MX, Ding B, Yu JY, Yan JH. Integrated solid-state Li-metal batteries mediated by 3D mixed ion-electron conductive anodes and deformable molten interphase. *Chem Eng J* **2022**;442:136227.
134. Chang J, Shang J, Sun YM, Ono L, Wang DR, Ma ZJ, Huang QY, Chen DD, Liu GQ, Cui Y, Qi YB, Zheng ZJ. Flexible and stable high-energy lithium-sulfur full batteries with only 100% oversized lithium. *Nat Commun* **2018**;9:4480.
135. Gao Y, Hu H, Chang J, Huang QY, Zhuang QN, Li P, Zheng ZJ. Realizing high-energy and stable wire-type batteries with flexible lithium-metal composite yarns. *Adv Energy Mater* **2021**;11:2101809.
136. Scheffler S, Poulin P. Piezoelectric fibers: processing and challenges. *ACS Appl Mater Interfaces* **2022**;14:16961.
137. Xu Q, Wen J, Qin Y. Development and outlook of high output piezoelectric nanogenerators. *Nano Energy* **2021**;86:106080.
138. Choi S, Ankonina G, Youn D, Oh S, Hong J, Rothschild A, Kim I. Hollow ZnO nanofibers fabricated using electrospun polymer templates and their electronic transport properties. *ACS Nano* **2009**;3:2623.
139. Du XX, Zhou Z, Zhang Z, Yao LQ, Zhang QL, Yang H. Porous, multi-layered piezoelectric composites based on highly oriented PZT/PVDF electrospinning fibers for high-performance piezoelectric nanogenerators. *J Adv Ceram* **2022**;11:331.
140. Yan JH, Han YH, Xia SH, Wang X, Zhang YY, Yu JY, Ding B. Polymer template synthesis of flexible BaTiO₃ crystal nanofibers. *Adv Funct Mater* **2019**;29:1907919.
141. Fu XP, Bu TZ, Li CL, Liu GX, Zhang C. Overview of micro/nano-wind energy harvesters and sensors. *Nanoscale* **2020**;12:23929.
142. Anwar S, Amiri M, Jiang S, Abolhasani M, Rocha P, Asadi K. Piezoelectric Nylon-11 fibers for electronic textiles, energy harvesting and sensing. *Adv Funct Mater* **2021**;31:2004326.
143. Wang J, Zhang Q, Cheng Y, Song FY, Ding YZ, Shao MW. Self-reinforced composites based on polypropylene fiber and graphene nano-platelets/polypropylene film. *Carbon* **2022**;189:586.
144. Pan CT, Wang SY, Yen C, Kumar A, Ku S, Zheng JL, Wen ZH, Singh R, Singh S, Khan M, Chaudhary R, Dai XF, Kaushik A, Wei DQ, Shiue Y, Chang W. Polyvinylidene fluoride-added ceramic powder composite near-field electrospun piezoelectric fiber-based low-frequency dynamic sensors. *ACS Omega* **2020**;5:17090.
145. Eom K, Shin Y, Kim J, Joo S, Kim K, Kwak S, Ko H, Jin JH, Kang S. Tailored poly(vinylidene fluoride-co-trifluoroethylene) crystal orientation for a triboelectric nanogenerator through epitaxial growth on a chitin nanofiber film. *Nano Lett* **2020**;20:6651.
146. Wang Z, He HY, Liu S, Wang H, Zeng QS, Liu Z, Xiong QH, Fan HJ. Air stable organic-inorganic perovskite nanocrystals@polymer nanofibers and waveguide lasing. *Small* **2020**;16:2004409.
147. Han Y, Jiang CL, Lin HC, Luo CH, Qi RJ, Peng H. Piezoelectric nanogenerators based on helical carbon materials and polyvinylidene difluoride-trifluoroethylene hybrids with enhanced energy-harvesting performance. *Energy Technol* **2020**;8:1901249.
148. Dong K, Peng X, Wang ZL. Fiber/fabric-based piezoelectric and triboelectric nanogenerators for flexible/stretchable and wearable electronics and artificial intelligence. *Adv Mater* **2020**;32:1902549.
149. Wang NZ, Daniels R, Connelly L, Sotzing M, Wu C, Gerhard R, Sotzing G, Cao Y. All-organic flexible ferroelectric nanogenerator with fabric-based electrodes for self-powered body area networks. *Small* **2021**;17:2103161.
150. Deng WL, Zhou YH, Libanori A, Chen GR, Yang WQ, Chen J. Piezoelectric nanogenerators for personalized healthcare. *Chem Soc Rev* **2022**;51:3380.
151. Su YJ, Li WX, Yuan L, Chen CX, Pan H, Xie GZ, Conta G, Ferrier S, Zhao X, Chen GR, Tai HL, Jiang YD, Chen J. Piezoelectric fiber composites with polydopamine interfacial layer for self-powered wearable biomonitoring. *Nano Energy* **2021**;89:106321.
152. Su YJ, Chen CX, Pan H, Yang Y, Chen GR, Zhao X, Li WX, Gong QC, Xie GZ, Zhou YH, Zhang SL, Tai HL, Jiang YD, Chen J. Muscle fibers inspired high-performance piezoelectric textiles for wearable physiological monitoring. *Adv Funct Mater* **2021**;31:2010962.
153. Li ZT, Wang ZL. Air/liquid-pressure and heartbeat-driven flexible fiber nanogenerators as a micro/nano-power source or diagnostic sensor. *Adv Mater* **2011**;23:84.
154. Soin N, Shah T, Anand S, Geng JF, Pornwannachai W, Mandal P, Reid D, Sharma S, Hadimani R, Bayramol D, Siores E. Novel, “3-D spacer” all fibre piezoelectric textiles for energy harvesting applications. *Energy Environ Sci* **2014**;7:1670.

Publisher's Note Springer Nature remains neutral with regard to jurisdictional claims in published maps and institutional affiliations.



Chuang Zhu is a Lecturer in the College of Textiles at Donghua University. He received his B.Sc. and Ph.D. degree from University of Manchester in Dr. Xuqing Liu's group. His research interest includes fiber surface modification, smart textiles and wearable electronics.



Jiawei Wu is currently a Ph.D. candidate under the supervision of Prof. Jianhua Yan in the College of Textiles at Donghua University. His research is in the development of micro-nano ceramic yarns.



Jianhua Yan is a professor in the College of Textiles at Donghua University. He received his Ph.D. degree from West Virginia University and then moved to Berkeley National Laboratory as a postdoc research fellow. His research is in the development of inorganic fiber materials and devices.



Xuqing Liu is a tenured research fellow, in the Department of Materials at the University of Manchester. He leads the Research group of Fiber Surface Molecular Engineering, and is the academic lead for Fiber Chemistry. His group utilizes the basic principles in chemistry, material science, and textiles, and fashion to enable novel applications and development of flexible stretchable electronics in energy devices and functional and sustainable fashion. He is the fellow of the Royal Society of Arts and the chairman of Chinese Textile and Apparel Society (CTAS-UK).